Title

A Quiescent Bcl11b High Stem Cell Population Is Required for Maintenance of the Mammary Gland

Journal

Cell Stem Cell, 20(2)

ISSN

1934-5909

Authors

Cai, Shang
Kalisky, Tomer
Sahoo, Debashis
et al.

Publication Date

2017-02-01

DOI

10.1016/j.stem.2016.11.007

Peer reviewed

HHS Public Access

Author manuscript

Cell Stem Cell. Author manuscript; available in PMC 2018 February 02.

Published in final edited form as:

Cell Stem Cell. 2017 February 02; 20(2): 247–260.e5. doi:10.1016/j.stem.2016.11.007.

A Quiescent *Bcl11b* High Epithelial Cell is Required for Mammary Gland Regeneration

Shang Cai[1], **Tomer Kalisky**[2,♫], **Debashis Sahoo**[1], **Piero Dalerba**[1], **Weiguo Feng**[3], **Yuan Lin**[3], **Dalong Qian**[1], **Angela Kong**[1], **Jeffrey Yu**[1], **Flora Wang**[1], **Elizabeth Y. Chen**[1], **Ferenc A. Scheeren**[1,3,♪], **Angera H. Kuo**[1], **Shaheen S. Sikandar**[1], **Shigeo Hisamori**[1,3], **Linda J. van Weele**[1], **Diane Heiser**[1], **Sopheak Sim**[1], **Jessica Lam**[1], **Stephen Quake**[2,♩], and **Michael F. Clarke**[1,4,*]

[1]Institute for Stem Cell Biology and Regenerative Medicine, School of Medicine, Stanford University, Stanford, CA, USA

[2]Department of Bioengineering, Stanford University School of Medicine, Stanford, CA 94305, USA

[3]Cancer Institute and Institute for Stem Cell Biology and Regenerative Medicine, Stanford University School of Medicine, Stanford, California, USA

Summary

Stem cells in many tissues sustain themselves by entering a quiescent state to avoid genomic insults and to prevent exhaustion caused by excessive proliferation. In the mammary gland, the identity and characteristics of quiescent epithelial stem cells are not clear. Here, we identify a quiescent mammary epithelial cell population expressing high levels of Bcl11b and located at the interface between luminal and basal cells. *Bcl11b*^{high} cells are enriched for cells that can regenerate mammary glands in secondary transplants. Loss of *Bcl11b* leads to a Cdkn2a-dpendent exhaustion of ductal epithelium and loss of epithelial cell regenerative capacity. Gain and loss of function studies show that *Bcl11b* induces cells to enter the G0 phase of the cell cycle and become quiescent. Taken together, these results suggest that *Bcl11b* acts as a central intrinsic regulator of mammary epithelial stem cell quiescence and exhaustion, and is necessary for long-term maintenance of the mammary gland.

eTOC summary

[*]Correspondence to: mfclarke@stanford.edu.
[4]Lead Contact
[♪]Department of Medical Oncology, Leiden University Medical Center, Leiden, The Netherlands
[♫]Faculty of Engineering, Bar-Ilan University, Ramat Gan 52900, Israel
[♩]Department of Surgery, Kyoto University, 54, Kawaharacho, Shogoin, Sakyoku, Kyoto, Japan 606-8507

Author Contributions

Conceptualization, S.C., M.F.C. and S.R.Q., Methodology, S.C., M.F.C., T.K.,W.F.,Y.L., F.A.S. Investigation, S.C., A.K.,J.Y.,F.W.,E.Y.C., S.S., J.L.,D.Q., Formal Analysis S.C., T.K., D.S., P.D., Data Curation D.S. and P.D. Writing-original draft, S.C. and M.F.C. Writing-Review&Editing W.F., Y.L., E.Y.C., A.H.K., S.S.S, L.J.v.W., D.H., S.H., Funding Acquisition M.F.C, S.C.

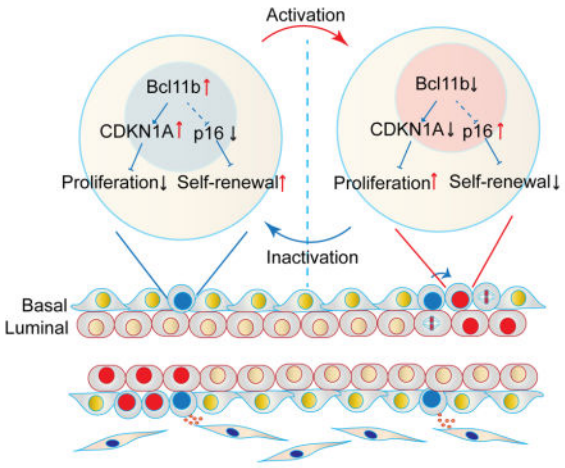

Cai et al. (2016) describe a quiescent mammary stem cell population labeled by *Bcl11b* and located at the luminal-basal interface that supports mammary gland regeneration. *Bcl11b* sustains this population by inducing cell cycle regulators that promote the dormant state.

Introduction

The mammary gland contains a ductal system consisting of basal and luminal cells that generates a milk-producing organ during pregnancy. Following weaning, the mammary gland ductal system undergoes involution and the proper long-term maintenance of the proliferation capacity of the mammary epithelia is required for multiple rounds of female reproductive cycles.

There are advantages provided by quiescence in tissue-specific stem cells; they may avoid proliferation associated genome damage that can cause the accumulation of deleterious mutations and/or the initiation of apoptosis (Codega et al., 2014; Foudi et al., 2009; Wilson et al., 2008). Despite extensive studies using a number of techniques including flow cytometry (Shackleton et al., 2006; Stingl et al., 2006), lineage tracing (Plaks et al., 2013; Rios et al., 2014; van Amerongen et al., 2012; Van Keymeulen et al., 2011; Wang et al., 2015), and *in vitro* culture (Prater et al., 2014; Zeng and Nusse, 2010), the cellular hierarchy of the mammary gland is still controversial. Some have suggested that the mammary gland is maintained by separate basal and luminal progenitors, while others have suggested a bipotent basal cell progenitor that can generate both basal and luminal cells (Rios et al., 2014; Van Keymeulen et al., 2011). Regardless of the hierarchy of the mammary epithelium, it is important to understand the molecular regulation of the long-lived epithelial cells, which have the greatest proliferation capacity.

For most of their life, quiescent stem cells (i.e. hematopoietic stem cells or skin stem cells) remain at minimal cycling rate and metabolic activities to preserve their long-term self-renewal ability under physiological condition. Upon stress or injury, they can be activated by growth signals and give rise to multiple cell types to orchestrate a homeostatic architecture of the organs for regeneration (Wilson et al., 2008). In the mammary gland, reminiscent of quiescent hematopoietic stem cells (HSCs), label retention assays suggest the existence of a

quiescent long-lived cell population with extensive self-renewal ability (dos Santos et al., 2013; Pece et al., 2010; Smith, 2005). Understanding the intrinsic molecular network that specifies the quiescence program of long lived mammary epithelial cells could shed light on the regulation of long-term tissue homeostasis, organ regeneration, cancer relapse, aging and many other pathological degenerative diseases.

In this study, through single cell gene expression analysis of mammary epithelia, we identified a quiescent population within mammary basal cells that expressed high level of *Bcl11b*. We demonstrated that *Bcl11b* is a major cell intrinsic factor that is functionally required for maintaining a minority of epithelial cells that express the basal cytokeratin *Krt17* in a dormant state. *Bcl11b* knockout mice had impaired mammary gland development and mammary epithelial cells were unable to regenerate mammary glands after transplantation. Thus, *Bcl11b* is required to preserve epithelial cell long-term proliferation capacity and to maintain normal mammary gland homeostasis.

Results

Bcl11b is a Nuclear Protein Highly Expressed in CD49f^{high}CD24^{med}Lineage^{-} Cells and Specifically Localized to the Mammary Duct Basal Layer

The composition of mammary epithelium at the single cell level was investigated. We first focused on CD49f^{high}CD24^{med}Lin^{-} cells, which are greatly enriched for mammary repopulating units (MRUs) as measured by transplantation assays (Shackleton et al., 2006; Stingl et al., 2006). To better understand the molecular regulation of long-term proliferation capacity as measured by transplantation assays, we isolated the various populations of mammary epithelial cells based on the expression of CD49f and CD24: Basal1 (CD49f^{high}CD24^{med}Lin^{-}) cells, which are enriched for cells with the greatest proliferation capacity, Basal2 (CD49f^{high}CD24^{low}Lin^{-}) and Lum1 (defined as CD49f^{low}CD24^{high}Lin^{-} cells), Lum2 (defined as CD49f^{low}CD24^{med}Lin^{-} cells) (Stingl et al., 2006) (Fig. 1A, S1A–C) were analyzed using sensitive single-cell multiplexed gene PCR (Dalerba et al., 2011). The expression of a number of transcription factors (which were selectively expressed by a subset of mammary epithelial cells) was screened in the CD49f^{high}CD24^{med}Lin^{-} population. In this screen, *Bcl11b*, a C2H2 zinc finger transcription factor and a member of various chromatin-remodeling complexes (e.g. SWI/SNF, NURD)(Cismasiu et al., 2005; Krasteva et al., 2012), was found to be highly expressed in a subset of Basal1 compared to Basal2 cells or luminal epithelial cells (Fig. 1A,B, S1C–F). Intriguingly, superimposed clustering analysis demonstrated that *Bcl11b* is not uniformly expressed at high levels in individual CD49f^{high}CD24^{med}Lineage^{-} cells (Fig. 1B). Instead, *Bcl11b* mRNA positive cells comprised only 4.8% of the Basal1 cells that expressed the basal cytokeratin *Krt17* (12 out of 248 cells) with both decreased frequency and levels of expression observed in Basal2 and luminal populations (Fig. 1C and S1A–D). This expression pattern was further confirmed by real time PCR analysis of the corresponding mammary populations (Fig. 1D). We couldn't detect Bcl11b expression in the overall luminal population, Cd14+ luminal progenitors, or Cd14- mature luminal cells (Fig. S1G).

Next, we examined the mammary tree for the location of the *Bcl11b* positive cells. In adult mice, immunofluorescence analysis showed that *Bcl11b* positive cells were sparsely

scattered within the interface of the basal and luminal cell layers of the duct in the mammary gland (Fig. 1E). Interestingly, *Bcl11b* positive cells were rarely seen in the basal cells of some ducts, which only had one layer of luminal cells and appeared to be mature (Fig. 1E). The immunochemistry corroborates the single cell gene expression data showing that Bcl11b is exclusively expressed by less than 1% of cells located at the interface of the basal and luminal cells.

To isolate *Bcl11b*^{high} cells from the mammary gland, we used a *Bcl11b* tdTomato reporter mouse (Li et al., 2010), which has an inserted IRES-tdTomato cassette at the 3'UTR of the *Bcl11b* locus (Fig. 1F). Consistent with the quantitative RT-PCR and immunochemistry results, a distinct population of tdTomato-high cells was exclusively restricted to cells adjacent to the basal population (Fig. 1G). Only a subset of the MRU-enriched CD49f^{high}CD24^{med}Lineage^{-} cells (5.7±3.5%, mean±S.D.) expressed high levels of *Bcl11b* as measured by tdTomato fluorescence intensity (n=24, $p<0.0001$) (Fig. 1H, I, S1H). These data suggested that CD49f^{high}CD24^{med}Lineage^{-} cells contain a minority population of cells that express high levels of *Bcl11b* RNA and protein. To track *Bcl11b* expression in intact mammary glands, *Bcl11b*$^{tdTomato/wt}$ reporter mice were analyzed by multi-photon microscopy. In these mice, individual cells expressing high levels of *Bcl11b* were sporadically distributed at the rim of the mammary gland, in the branching mammary tips, bifurcating ends, and scattered in the mature ducts (Fig. 1J). Thus, single cell gene expression, immunofluorescence, flow cytometry and live cell imaging all corroborated the rarity of *Bcl11b*^{high} cells are located adjacent to both the basal and luminal cells in the mammary ducts.

Conditional Knockout of *Bcl11b* Impairs Mammary Gland Development and Regeneration Capacity

The fact that *Bcl11b* is an epigenetic regulator of transcription and a potential fate determinant prompted us to further investigate whether *Bcl11b* played a functional role in the mammary epithelium and mammary gland development. We deleted *Bcl11b* expression in the mammary gland by crossing Krt14-cre mice with *Bcl11b*$^{flox/flox}$ mice (Golonzhka et al., 2009). Embryonically activated Krt14-cre can trace the majority of the mammary epithelia including both luminal and basal cells, allowing us to investigate *Bcl11b*'s global function within the mammary gland. Analysis of the *Bcl11b* mutant mammary gland showed substantially retarded postnatal development with significant reductions (~50%) in mammary tree size ($p<0.001$) (Fig. 2A, B). This suggests that *Bcl11b* is required for proper mammary morphogenesis.

To specifically interrogate *Bcl11b* null cells, we crossed Krt14-cre *Bcl11b*$^{flox/flox}$ mice with an mTmG reporter mouse to label the cells that had expressed cre. Consistent with previously reported analyses of Krt14-cre mice, our control mammary gland (Krt14-cre *Bcl11b*$^{wt/wt}$ mTmG) showed predominantly green ducts (cre+) and a small amount of red epithelia (cre-) (Fig. 2C, top panel). Interestingly, in the mutant (Krt14-cre *Bcl11b*$^{flox/flox}$ mTmG) mice, the mammary glands showed a dramatic reduction in green cells with a striking increase in observable red epithelia, suggesting that these mammary ducts were made up of a significant number of cells that had escaped *Bcl11b* deletion by cre (Fig. 2C,

bottom panel). When quantified by flow cytometry, the percentage of green cells in the mammary epithelia dropped from 84.4±5.0% (mean±SD; n=4) in the control mouse to 34.3±15.77% (mean±SD; n=5) in the mutant mouse ($p<0.001$; Fig. 2D, E).

In addition, the green cell reduction trend also held true in both basal and luminal mammary subpopulation (Fig. 2E). This data suggests that the *Bcl11b* null cells had a reduced ability to maintain the mammary gland compared to their wild type counterparts. Interestingly, Bcl11b knockout affected the luminal cells (which do not express detectable levels of Bcl11b) more dramatically than the basal cells. This suggests that the Krt14 positive cells had impaired ability to give rise to luminal cells after Bcl11b deletion, reminiscent of a defect in lineage commitment and multi-potency at some time during the mammary gland development.

We speculated that the impaired mammary gland of *Bcl11b* knockout mice resulted from a proliferation defect. Hence, we tested the mammary tree reconstitution capacity of *Bcl11b* mutant cells by limiting dilution transplant. Indeed, *Bcl11b* embryonic deletion caused a 75% reduction of the total MRUs in *Bcl11b* null mammary cells compared to wild-type mammary cells (Fig. 2F). When we passaged the primary outgrowths to secondary recipient mice, the *Bcl11b* mutant cells were unable to regenerate new mammary trees (Fig. 2G, S2A). Together, these data suggest embryonic deletion of *Bcl11b* impairs the long-term regeneration capacity, and results in a gradual exhaustion of the mammary epithelium.

To ask whether *Bcl11b* plays a role in maintaining the regeneration capacity of the adult mammary epithelia, adenovirus-cre was used to abruptly and efficiently knock-out *Bcl11b* due to high transient expression of cre (Russell et al., 2003). Since adenovirus will not integrate into the genome, the temporary cre activity will not permanently injure the cells. Taking advantage of this property of adenoviruses, mammary cells isolated from $Bcl11b^{wt/wt}$ and $Bcl11b^{flox/flox}$ mice were infected with adeno-cre-GFP. GFP+ mammary epithelial cells were isolated by sorting and transplanted into recipient mice (Fig. S2B). Analysis of the recipients' mammary fat pads revealed a prominent reduction (~20 fold) of mammary repopulating activity in *Bcl11b* knockout versus wild-type cells ($N=3$, $p<0.01$; Fig. 2H–J and Table S1). This indicates that when *Bcl11b* is efficiently deleted in adult mammary gland, the regeneration capacity of adult MRUs is significantly impaired. These data reinforce the hypothesis that *Bcl11b* is necessary for the maintenance of adult mammary gland epithelium.

Bcl11b^{high} Cells are Highly Competent in Mammary Gland Reconstitution

Since *Bcl11b* is expressed in a subset of mammary cells and is required for mammary gland reconstitution, we were intrigued by the biology of $Bcl11b^{high}$ cells. The proliferation capacity of $Bcl11b^{high}$ $CD49f^{high}CD24^{med}Lin^{-}$ cells was determined using *in vitro* and *in vivo* assays. First, $Bcl11b^{high}$ and $Bcl11b^{low}$ $CD49f^{high}CD24^{med}Lineage^{-}$ cells were isolated from the $Bcl11b^{tdTomato/wt}$ reporter mouse and subsequently cultured on matrigel using culture conditions enabling the growth of murine MRUs (Zeng and Nusse, 2010). $Bcl11b^{high}$ cells formed ~8 fold more colonies than their $Bcl11b^{low}$ counterparts (Fig. 3A), which indicates that cells with the highest expression of *Bcl11b* are greatly enriched for cells with the ability to form colonies of mammary epithelial cells. Furthermore, the

Bcl11b^{high}CD49f^{high}CD24^{med}Lin^{-} population has *in vitro* developmental potential, as colonies formed from a single *Bcl11b*^{high} cell clearly contain both basal and luminal epithelia in the single cell gene expression analysis (Fig. S3A, B). These data suggest that *Bcl11b*^{high} cells maintain their proliferation potential in the in vitro organoid cultures.

Next, we investigated whether *Bcl11b*^{high} CD49f^{high}CD24^{med}Lineage^{-} cells have reconstitution activity. We transplanted *Bcl11b*^{high} and *Bcl11b*^{low} CD49f^{high}CD24^{med}Lineage^{-} cells into syngeneic mice. Consistent with the colony formation assay, *Bcl11b*^{high}CD49f^{high}CD24^{med}Lineage^{-} cells displayed a 6-fold enrichment in their capacity to engraft mice over *Bcl11b*^{low} cells ($p<0.05$, N=3) (Fig. 3B, and Table S2). Single cell transplants of *Bcl11b*^{high} CD49f^{high}CD24^{med}Lineage^{-} into syngeneic mice revealed an engraftment frequency of 1/9.5 (4 outgrowths of 38 single cell injections; Fig. 3C–E). In addition, the outgrowths generated from *Bcl11b*^{high} CD29^{high}CD24^{med}Lineage^{-} cells can be efficiently passaged and reconstitute new mammary trees in a secondary transplant (Fig. 3F). These data suggest that *Bcl11b* directly regulates the long-term regeneration ability of mammary cells rather than indirectly affecting mammary gland development through a cell extrinsic mechanism.

Bcl11b^{high} Cells are Quiescent

For many somatic tissues, stem cells utilize a strategy of switching between an active proliferating state and a resting state to preserve long-term regeneration potential (Adorno et al., 2013; Fuchs, 2009; Wilson et al., 2008). Actively proliferating mammary progenitors were recently identified by the cell surface marker Procr. We were therefore intrigued by the relationship between *Bcl11b*^{high} and Procr^{high} mammary cells. Interestingly, FACS analysis showed that *Bcl11b* and Procr marked two distinct populations of CD49f^{high}CD24^{med}Lin^{-} that do not overlap but are instead mutually exclusive (Fig. 4A), which is further supported by our single cell gene expression analysis (Fig 4B). This led us to dissect the cellular status of these two distinct populations. DNA content analysis of these two populations showed that 11% of Procr^{high} CD49f^{high}CD24^{med}Lin^{-} were actively proliferating with cells in 4N fraction while less than 1% of the *Bcl11b*^{high} CD49f^{high}CD24^{med}Lin^{-} were in the 4N fraction (Fig. 4A). This was further corroborated by an EdU incorporation assay (only labels replicating cells), which showed that *Bcl11b*^{high} cells did not incorporate any EdU (Fig. 4C). To determine whether *Bcl11b*^{high} cells are in G_1 or G_0, we co-stained a 12-week old mouse mammary glands with *Bcl11b* and the proliferation antigen, Ki67; Ki67 is expressed by actively proliferating cells throughout the cell cycle, but not by cells in G_0. Analysis of *Bcl11b* and Ki67 co-localization revealed that the two genes were rarely expressed in the same cells in both ducts and terminal end buds (Fig. 4D, E).

This was further bolstered by an unbiased single cell gene expression analysis on *Bcl11b* and Ki67 mRNA expression in adult mouse mammary gland (Fig. 4F and S4A). As a second hallmark of G_0 cells, quiescent stem cells have a low RNA content and can be identified as a Pyronin Y^{low}-Hoechst^{low} population (Gothot et al., 1997). To confirm *Bcl11b*^{high} cells are slow cycling, we sorted CD49f^{high}CD24^{med}Lin^{-} that were Pyronin Y^{high} Hoechst^{high}(G_2), Pyronine^{high}Hoeschst^{low} (G_1) or Pyronin Y^{low}-Hoeschst^{low} (G_0) and subjected them to real-time PCR analysis for *Bcl11b*. As predicted, *Bcl11b* was highly expressed in the Pyronin

Y^{low}-$Hoechst^{low}$ population, which are the putative G_0 cells (Fig. 4G). To ask whether *Bcl11b* expression is closely related to phenotypic slow cycling cells, we performed a long label-retaining assay in breast organoid cultures using the membrane dye PKH26 (Pece et al., 2010). Our result revealed *Bcl11b* is consistently enriched by ~3 fold in the $PKH26^{high}$ population (Fig. 4H, I). Recently, *in vivo* long label retaining assay using an induced H2B-GFP identified a cell surface protein Cd1 as a marker for long label retaining cells (LRCs) (dos Santos et al., 2013); hence, we isolated Cd1+ and Cd1- basal cells. We found that Bcl11b was consistently enriched about 5 fold in the Cd1+ population compared with the Cd1- population (Fig. S4B). These data collectively demonstrate that the vast majority of $Bcl11b^{high}$ cells are G_0 label-retaining cells with a reduced rate of proliferation, both *in vivo* and *in vitro*.

Bcl11b Functionally Regulates Quiescence of Mammary Epithelial Cells

As transcription factors often determine a specific expression profile, gain and loss of function assays were done to address whether *Bcl11b* itself regulates the cycling rate of $CD49f^{high}CD24^{med}Lin^{-}$ cells. We found that enforced expression of *Bcl11b* significantly repressed colony growth of $CD49f^{high}CD24^{med}Lineage^{-}$ cells (Fig. S4C, D). To eliminate the possibility that this was an overexpression artifact, we constructed an inducible *Bcl11b* vector using the Tet-on system to fine tune induced *Bcl11b* expression levels. In the murine mammary epithelial Comma D β cell line (Deugnier et al., 2006), which has a heterogeneous expression of *Bcl11b* (Fig. S5), induced *Bcl11b* expression dramatically repressed proliferation (Fig. S4E). Next, we investigated the effects of *Bcl11b* overexpression in $CD49f^{high}CD24^{med}Lineage^{-}$cells using a competition growth assay. We mixed pInducer-*Bcl11b* transduced $CD49f^{high}CD24^{med}Lineage^{-}$ cells (GFP+) with untransduced $CD49f^{high}CD24^{med}Lineage^{-}$ cells (GFP-) in a 1:1 ratio and cultured them in the presence or absence of Doxycycline (Fig. 5A–C). Doxycycline-induced *Bcl11b* expression strikingly reduced the percentage of GFP positive cells from 43% in the control cells to 11% in the *Bcl11b*-induced cells ($p<0.01$; Fig. 5A–C). The inhibition of $CD49f^{high}CD24^{med}Lineage^{-}$ cell growth is not an artifact of the construct or Doxycycline, as the overexpression of a control transcription factor (Nr2f1) caused an opposite phenotype of increased proliferation after induced expression (Fig. 5A–C). These data suggest that *Bcl11b* functionally suppresses mammary cell proliferation.

To elucidate how *Bcl11b* is involved in the cell cycle, we performed microarray gene expression analysis of control and *Bcl11b*-induced cells. Gene enrichment analysis showed that cells expressing low levels of *Bcl11b* (DOX- uninduced) were significantly enriched for G_2 pathway factors and the pre-replicative complex subunits, which are required for DNA duplication (Fig. S6A). Moreover, genes required for G_1 progression, including Ccnd1, Ccne1, Ccne2, Cdk2, Cdk6, E2f1, were also strikingly enriched in *Bcl11b*-uninduced cells (Fig. S6B). Notably, mKi67, which distinguishes G_1 and G_0, was significantly down regulated by *Bcl11b* (Fig S6B). To ensure these results were not unique to the Comma D β cell line, this gene down-regulation pattern was confirmed by real time PCR of cells from FACS sorted primary $CD49f^{high}CD24^{med}Lin^{-}$ cells (Fig. S6E, F). This gene expression analysis suggests that *Bcl11b* is targeting genes that regulate the early G_1 phase of the cell cycle to prevent cell cycle progression. Consistent with this idea, we also observed up-

regulation of cell cycle repressors such as Foxo1, Foxo3 and Foxo4, in the *Bcl11b*-induced cells (Fig. S6C). The Foxo factors repress cell cycle in part via repression of expression of Cyclin D (Schmidt et al., 2002). Notably, we found that Sall2, a gene required for serum-starvation induced proliferation arrest (Liu et al., 2007), was up-regulated upon *Bcl11b* expression (Fig. S6C). These data suggest that *Bcl11b* systemically and consistently inhibits G_1–G_2 cell cycle progression, which induces mammary cells into a quiescent state (Fig. S6D).

To ask whether *Bcl11b* plays a role in the maintenance of the quiescent mammary cells, we measured the proliferation of *Bcl11b*-loss of function CD49f^{high}CD24^{med}Lineage^{-} cells (Krt14-cre *Bcl11b*$^{fl/fl}$) in an organoid assay. The *Bcl11b* loss of function cells produced colonies that were 50% larger compared to their wild type counterparts (Fig. 5D–G). When we induced the depletion of *Bcl11b in vivo* with a Rosa26-creERT2 *Bcl11b*$^{fl/fl}$ mTmG mouse, the basal cells of the *Bcl11b* null population (GFP+) exhibited a significant expansion over that of the *Bcl11b* wild type population (GFP−) (Fig. 5H). These gain and loss of function experiments strongly suggest that *Bcl11b* is required for maintaining CD49f^{high}CD24^{med}Lin^{-} cells in a quiescent state.

Since it has been recently reported that steroid hormones tightly regulate the reconstitution activity of mammary cells during estrus cycle and pregnancy (Asselin-Labat et al., 2010; Joshi et al., 2010), we asked whether hormones regulates Bcl11b. We first isolated mammary basal cells at various stages of mouse pregnancy, and subjected them to quantitative PCR analysis. Interestingly, we found a prompt increase of Ki67 expression at early pregnancy followed by a deep decline in the later pregnancy. In contrast, Bcl11b expression gradually decreased throughout the full term of pregnancy, suggesting that epithelial cells downregulated Bcl11b to allow drastic proliferation followed by differentiation (Fig 5I). To ask whether the decrease of Bcl11b during pregnancy is due to elevation of hormones, we treated ovariectomized mice with estrogen and progesterone. Indeed, Bcl11b's level was consistently downregulated to a similar level in pregnancy (Fig. 5J). These data suggest that steroid hormones act to downregulate Bcl11b in the Bcl11b high cells to promote the expansion of mammary epithelial cells.

Bcl11b Regulates CD49f^{high}CD24^{med}Lin^{-} cells Homeostasis via Cdkn1a and Cdkn2a

The G_1 phase of the cell cycle is tightly regulated by cyclin dependent kinase inhibitors (CDKIs) through inhibition of kinase activity of the cyclinD/CDK4/6 and cyclinE/CDK2 complexes. Certain CDKIs have been reported to reduce proliferation of stem cells in certain tissues (Cheng et al., 2000; Kippin et al., 2005; Matsumoto et al., 2011; Zou et al., 2011). We sought to investigate the possibility that *Bcl11b* inhibits proliferation by regulating CDKIs. We performed real time PCR for all the CDKIs using samples from the competitive growth assay. We found that upon *Bcl11b* induction, Cdkn1a/p21 mRNA was up-regulated, while other CDKIs showed only minor or insignificant changes (Fig. 6A, B). p21 has been shown to retard both hematopoietic stem cell and neural stem cell proliferation (Cheng et al., 2000),(Kippin et al., 2005; Marques-Torrejon et al., 2013). Recently, using a Cdk2 sensor, p21 was shown to be responsible for reducing proliferation in multiple epithelial cell lines (Spencer et al., 2013). We reasoned that if *Bcl11b* exerted cell cycle repression through p21,

knockout of p21 should impair *Bcl11b*'s ability to repress CD49f^{high}CD24^{med}Lin^{-} proliferation. To test this, we performed a competition growth assay with CD49f^{high}CD24^{med}Lin^{-} using a p21 knockout mouse. Induction of *Bcl11b* did not repress cell growth as efficiently in the p21 mutant cells as in wild-type cells (Fig. 6C). The reduced proliferation of the GFP positive cells was partially rescued (11.74±1.1% GFP positive cells in Dox+ WT vs 19.0±2.0% GFP positive cells in Dox+ p21 mutant, $p<0.01$). This data suggests that p21 is one of the pathways that *Bcl11b* regulates to control the cell cycle.

In certain somatic tissues it has been shown that a significant proportion of the tissue stem cells are slow cycling. For example, HSCs need to remain in the slow cycling state to maintain self-renewal ability (Essers et al., 2009; Wilson et al., 2008). Over-proliferation after various genetic perturbations or tissue damage by insults such as toxins, often leads to stem cell exhaustion *in vivo* and cellular senescence *in vitro*, mediated by either the p53 or INK4a (Cdkn2a) pathway (Beausejour et al., 2003; Lin et al., 1998; Schmitt et al., 2002). We asked whether *Bcl11b* knockout-mediated mammary exhaustion is dependent on the p53 or Cdkn2a pathways. To test whether *Bcl11b* has any correlation with Cdkn2a and p53 expression, we applied a boolean analysis (Sahoo et al., 2008) to a pool of >10,000 published mouse microarray datasets from GEO. Interestingly, the expression of *Bcl11b* was mutually exclusive to that of both p53 and Cdkn2a (Fig. 6D–E; $S_{Bcl11b\text{-}Cdkn2a}=9.45>3$, $ER_{Bcl11b\text{-}Cdkn2a}=0.05<0.1$; S: Boolean Statistics, ER: Error Rate), suggesting that there might be a direct or indirect molecular link between *Bcl11b* and the Cdkn2a or p53 pathways.

To test whether Cdkn2a and/or p53 are biologically important for *Bcl11b* function, we constructed lentiviral p53 shRNA and Cdkn2a shRNA vector (Adorno et al., 2013), and knocked down these two genes in the *Bcl11b* knockout (adenovirus-cre mediated) mammary epithelia. We subsequently transplanted these cells into recipient mice. Limiting dilution transplant analysis showed that p53 knockdown did not change the MRU frequency compared with *Bcl11b* knockout alone. However, Cdkn2a knockdown significantly increased MRU frequency by ~3 fold ($p<0.05$; Fig. 6F, G and Table S3). This data suggests that the MRU defect in the *Bcl11b* mutant mice is mediated at least in part by the Cdkn2a pathway. Since Cdkn2a has been linked to impaired stem cell function and senescence add Park nature Bmi1 paper reference (Park et al., 2003; Sato et al., 2015; Sharpless, 2004), our data suggest loss of *Bcl11b* might result in MRU and mammary gland exhaustion via the Cdkn2a senescence pathway.

Discussion

In this study, we have identified a dormant population of mammary epithelial cells that are important for normal mammary gland homeostasis. These cells rely on *Bcl11b* to maintain quiescence. *Bcl11b* is necessary for the long-term maintenance of the mammary gland at least in part via prevention of a Cdkn2a-mediated mammary epithelial cell exhaustion. Most other genes that have been linked to maintenance of the mammary epithelium such as *Bmi1* and *Bcl11a* are expressed by a larger percentage of both the luminal and basal cells in the mammary epithelium (Khaled et al., 2015; Pietersen et al., 2008). By contrast, only a small number of mammary epithelial cells that express the basal cytokeratin *Krt17* also express

detectable levels of *Bcl11b* mRNA or protein as measured by immunochemistry (Fig.1E) or quantitative single cell RT-PCR (Fig.1B). These results suggest that basal epithelial cells must cycle into a quiescent, *Bcl11b*^{high} state in order to maintain a normal mammary gland.

In many somatic organ systems, stem cells have to fulfill seemingly opposing demands of rapid proliferation to produce the mature, functional cells of the organ/tissue, while also cycling slowly in order to preserve long-term regenerative potential(Harmes and DiRenzo, 2009). The mechanism of maintaining a slow cycling quiescent state is the key to understand how cells coordinate these two demands. In the hematopoietic system, HSCs rely on p21 (Cheng et al., 2000) and p57 (Matsumoto et al., 2011) to be maintained at the quiescent state and can be activated by IFNa (Essers et al., 2009). In the mammary gland, slow cycling mammary cells with the ability to gain extensive proliferative capacity have been identified by many approaches including BrdU-labeling (Bussard et al., 2010; Smith, 2005), PKH26 labeling *in vitro* (Pece et al., 2010), and H2B-GFP pulse chasing (dos Santos et al., 2013). However, neither the intrinsic molecular network that regulates the proliferation state of mammary epithelial cells or the biological consequences of the slow cycling state is fully understood. In this study, we have identified the nuclear factor *Bcl11b* as a central regulator of the proliferation state of CD49f^{high}CD24^{med}Lineage^{-} cells. Loss of function studies show that *Bcl11b* plays an essential role in maintaining CD49f^{high}CD24^{med}Lineage^{-} cells' regenerative capacity. At the same time, *Bcl11b* induces basal epithelial cells to enter a ki67 negative, G_0 state. We further show that loss of *Bcl11b* results in exhaustion of the mammary epithelium at least in part dependent on Cdkn2a, which is known to regulate senescence programs in many tissues including stem cells and contribute to tissue degeneration in aging in many tissues including the mammary gland (Adorno et al., 2013; Krishnamurthy et al., 2006; Pietersen et al., 2008; Pustavoitau et al., 2016). In contrast, induced *Bcl11b* expression activates the G1 cell cycle inhibitor p21. Thus, our data identify *Bcl11b* as a crucial component of the molecular mechanism by which mammary epithelia are maintained long term, in part by evading the Cdkn2a senescence program and entering the Cdkn1a dependent quiescence program.

There are several models of the adult mammary epithelial cell hierarchy (Rios et al., 2014; Van Keymeulen et al., 2011), and our results could be explained by any of the postulated mammary gland hierarchy models. For example, it is possible that the Bcl11b high cells are the true stem cell. A second model is that induction of Bcl11b induces a *Krt17*$^{+}$ cell to enter a stem cell state. A third model is that induction of Bcl11b induces any mammary epithelial cell to enter a "stem cell state'. There are many other possible models. Regardless of which mammary gland hierarchical model is correct, our data clearly show that Bcl11b is essential for long term maintenance of the ductal epithelium and maintenance of long-term proliferation capacity.

Normal stem cells are thought to be targets for oncogenic transformation and stem cell programs are often used by cancer cells (Behjati et al., 2014; Jamieson et al., 2004; Jan et al., 2012; Shimono et al., 2009). As quiescent mammary cells are a long-lived population, they could be a prime targets for successive and accumulative genomic alterations, ultimately causing malignant transformation. Therefore it will be interesting to dissect the dynamics of this quiescent population during carcinogenesis to determine whether these

cells play a role in tumorigenesis. For example, dormant cancer cells are often resistant to cytotoxic agents that mainly target proliferating cells, resulting in increased risk of cancer relapse and metastasis; thus it is imperative to determine whether BCL11B regulates quiescence in breast cancer and contributes to therapy resistance. If so, the elucidation of how BCL11B regulates quiescence could reveal novel therapeutic targets for breast cancer.

STAR Methods

CONTACT FOR REAGENT AND RESCOURCE SHARING

Further information and requests for reagents may be directed to, and will be fulfilled by the corresponding author Michael F. Clarke at Institute for Stem Cell Biology and Regenerative Medicine (ISCBRM), Stanford University. Email: mfclarke@stanford.edu

EXPERIMENTAL MODEL AND SUBJECT DETAILS

Animal studies—The $Bcl11b^{flox/flox}$ mice (C57/BL6 background) were generously provided by Mark Leid's lab, and were described previously (Golonzhka et al., 2009). The $Bcl11b^{tdtomato}$ knock-in mice were generously provided by Pentao Liu's lab, and were described previously (Li et al., 2010). The mTmG (stock number 007676), Krt14-cre mice (stock number 018964) Cdkn1a KO mice (stock number 016565) were purchased from Jackson Laboratory. For analysis of pubertal mammary gland, 4–6weeks female mice were used. For experiments of Bcl11b KO whole mount, limiting dilution transplant, MRU sorting, competition growth assay and immunofluorescence staining, adult female mice (8–16weeks) were used. For each experiment, the age of the female mice used was indicated in the text. All animal procedures were conducted in accordance with a protocol approved by the Stanford University APLAC committee. Mice were maintained in house under aseptic sterile conditions. Mice were administered with autoclaved food and water.

Cell lines—Comma D beta cell line was kindly provided by Dr. Medina, and was described previously (Campbell et al., 1988). Comma D beta cell line was cultured in DMEM-F12 (Invitrogen) supplemented with 2% of Fetal Bovine Serum (Hyclone), 1% PSA (Invitrogen), 10ng/ml EGF(BD) and 5 μg/ml Insulin (Sigma), at 37 degree with 5% CO2.

METHOD DETAILS

Tissue Processing and Flow Cytometry—The 2^{nd},3^{rd},4^{th} pair of mammary glands from 8–16 week old virgin C57/BL6 mice were dissected and processed according to the published protocol (Prater et al., 2013) with minor revision. Mammary gland were manually and mechanically minced into 1mm size and digested with 0.5mg/ml Collagenase and 50U/ml hyaluronidase (Stem Cell Technology) for 2 hrs with gentle pipetting every 30mins. Digested mammary homogenate was spun down at 1500 rpm in Allegra^{TM} 6KR Centrifuge (Beckman Coulter), followed by 5ml ACK lysing buffer (Lonza) treatment for 5min on ice to remove erythrocytes. Then, mammary cells were digested by 5ml 0.25% Trypsin-EDTA (Gibco) for 2–5min, followed by brief DNase I (Worthington) plus Dispase (Stem Cell Technologies) digestion. Dissociated mammary cells were filtered by 40 μm strainer to obtain single cell suspension. For FACS analysis, mammary single cells were stained with CD45 (Biolegend), CD31 (Biolegend), Ter119 (Biolegend), CD49f (Biolegend), EpCAM

(Biolegend), CD24 (Biolegend), CD14(Biolegend), CD1d(Biolegend), Procr (Ebioscience) with appropriate conjugated fluorophores for 15min on ice. Then cells were washed and resuspended in HBSS+2%FBS+PSA+DAPI (1ug/ml) at a density of 5 million/ml. Stained samples were analyzed and sorted on FACS Aria II (BD Bioscience) with 100um or 130um nozzle.

Mammary Colony Formation Assay—L1-wnt3A feeder cells (generous gift from Roel Nusse lab) were administered a 40Gy dose of X-ray irradiation, and plated in 96 well plate at a density of 10k/well for 4hrs to allow stable attachment. 30ul of growth factor reduced Matrigel (BD Bioscience) was then overlaid on top of the feeder cells and solidified at 37degree for 10min. 1K/well CD49f^{high}CD24^{med}Lin^{-} cells were resuspended in 200ul culture media (DMEM F12+2% FBS+PSA+B27+10mM HEPES) supplemented with EGF (10ng/ml, BD Bioscience), Rspo1(250ng/ml, R&D), ROCK inhibitor Y27632 (10uM, Sigma), and Noggin (100ng/ml, R&D), and were overlaid on top of the matrigel. Plate was maintained in 37 degree incubator at 5% CO2 for 1–2 weeks. Single cell colony formation analysis was performed in the same condition.

Real Time PCR—500–2000 primary mammary cells or Comma D beta cells of various mammary populations were directly sorted into Eppendorf tube containing 400ul Trizol (Life Technologies). RNA was extracted according to the manufacturer's instruction with addition of ultrapure glycogen (Life Technologies) as carrier. RNA was reverse transcribed to cDNA using SuperScript III First Strand Synthesis kit (Life Technologies) according to the manufacturer's instructions. cDNA was preamplified 15–20 cycles according to the cell number using SybrGreen mastermix (Applied Biosystems) and target gene primer pool designed by IDT (Integrated DNA Technologies). Preamplified cDNA was then subjected to the real time PCR for specific gene target according to manufacturer's instructions using 7900HT Real Time PCR system (Applied Biosystems). Data were analyzed by SDS2.4 software and Excel. Sybrgreen primers are listed below: *Bcl11b*: Forward AGGAGAGTATCTGAGCCAGTG, Reverse GTTGTGCAAATGTAGCTGGAAG; p21: Forward CTTGCACTCTGGTGTCTGAG Reverse GCACTTCAGGGTTTTCTCTTG; Ki67: Forward TGCCCGACCCTACAAAATG Reverse GAGCCTGTATCACTCATCTGC; p16: Forward GTGCGATATTTGCGTTCCG Reverse TCTGCTCTTGGGATTGGC; p57: Forward CGCAAACGTCTGAGATGAGTTAG Reverse TCCTGCTACATGAACGAAAGG; p19: Forward CTTCATCGGGAGCTGGTG Reverse AGGCATCTTGGACATTGGG; Cdc25a: Forward TCCATCCCAGTCTCTATCCC Reverse TCAAATCCTGATGCTTCCCAG; Cdk1: Forward TGCAGGACTACAAGAACACC Reverse GCCATTTTGCCAGAGATTCG; Cdk2: Forward GCATTCCTCTTCCCCTCATC Reverse GGACCCCTCTGCATTGATAAG; Cdc25c: Forward GCAAACCTAAGCATTCTGTCG Reverse CAGAGGTCCAGATGAATCCAAG; Wee1: Forward GATCTCCTTTTGCAAGTTGGC Reverse CCAGTCATCTTCATCTCCTTCC; Foxo1: Forward CTACGAGTGGATGGTGAAGAG Reverse TGTGAAGGGACAGATTGTGG; Foxo4: Forward CTACTTCAAGGACAAGGGTGAC Reverse TGCAAGGACAGGTTGTGAC; Top2a: Forward AGTCAGACGTGAGCAGTAATG Reverse CTTCATCCTCATCCTTCTCATCC

Single Cell Gene Expression Analysis—Single-cell gene-expression experiments were performed using Fluidigm's M48 quantitative PCR (qPCR) DynamicArray microfluidic chips (Fluidigm) as described (Dalerba et al., 2011). Single cells were sorted by FACS into individual wells of 96-well PCR plates. Each 96-well plate was preloaded with 5 μl/well of CellsDirect PCR mix (Life Technologies) and 0.1 μl/well (2 U) of Superase In RNase-inhibitor. Following single-cell sorting, each well was supplemented with 1 μl of SuperScript-III RT/Platinum Taq (Life Technologies), 1.5 μl of Tris-EDTA (TE) buffer and 2.5 μl of a mixture of 48 pooled TaqMan assays (Applied Biosystems) containing each assay at 1:100 dilution. Single-cell mRNA was directly reverse transcribed into cDNA (50 °C for 15 min, 95 °C for 2 min), pre-amplified for 20 cycles (each cycle: 95 °C for 15 s, 60 °C for 4 min) and diluted 1:3 with TE buffer. A 2.25 μl aliquot of amplified cDNA was then mixed with 2.5 μl of TaqMan Universal PCR Master Mix (Applied Biosystems) and 0.25 μl of Fluidigm's “sample loading agent,” then inserted into one of the chip “sample” inlets. Individual TaqMan assays were diluted at 1:1 ratios with TE. A 2.5 μl aliquot of each diluted TaqMan assay was mixed with 2.5 μl of Fluidigm's “assay loading agent” and individually inserted into one of the chip “assay” inlets. Samples and probes were loaded into M48 chips using an IFC Controller HX (Fluidigm), then transferred to a BioMark real-time PCR reader (Fluidigm) following manufacturer's instructions. The Taqman probes used in this paper were purchased from Applied Biosystems (Life Technologies) and are listed below: Krt 17: Mm01306857_mH, ActB: Mm00607939_s1, *Bcl11b*: Mm00480516_m1, Cldn3: Mm01196233_s1, Gapdh: Mm03302249_g1, Krt8: Mm00835759_m1, Krt18: Mm01601702_g1, EpCAM: Mm01227384_m1, Krt19: Mm00492980_m1, Itga6: Mm01333831_m1, Itgb1: Mm00690415_g1, Cd44: Mm01277161_m1, Acta2: Mm00725412_s1, Snai2: Mm00441531_m1, Gata3: Mm00484683_m1, Foxo1: Mm00490671_m1, Axin2: Mm01265783_m1, Ezh2: Mm00468449_m1, Bmi1: Mm03053308_g1, Dll1: Mm00432841_m1, EGFR: Mm01187857_m1, Krt5: Mm00503549_m1, Mme: Mm01285048_m1.

Western Blot—100k Comma D beta cells were lysed by 2X Laemmli SDS sample buffer (100mM Tris pH6.8, 10% glycerol, 4% SDS, 0.01% Bromophenol Blue), and boiled on heat block at 100 degree for 15min. Samples were loaded to 4%–20% precast gradient gel (Bio-Rad) and electrophoresed at 200v for 45min, and transferred to Odyssey® nitrocellulose membrane (LI-COR). Membrane was blocked by PBS+0.1% tween 20+5% Non-fat dry milk for 1hrs RT, and then subjected to primary antibody staining beta Actin (Santa Cruz) 1:500, Rat anti *Bcl11b* 25B6 (Abcam) 1:1000 1hrs RT or 4 degree overnight. Membrane was then washed by PBST (PBS+0.1% Tween 20) 4X5min, and stained with secondary antibodies HRP-Donkey anti mouse, rat, or rabbit (GE Healthcare) 1:10,000 RT 1hr. Membrane was subsequently washed 4X10min by PBST and developed using SuperSignal® West Dura Extended Duration Substrate (Thermo Scientific) and KODAK X-OMAT LS film (KODAK).

Immunofluorescence—For frozen section, mammary gland was dissected and immediately fixed by 10% formalin for 1hrs followed by PBS washing and 30% sucrose infiltration overnight. The fixed mammary tissue was then embedded in O.C.T. compound (Tissue-Tek) and frozen in −80 degree. Frozen tissue block was sectioned to 14 um at

−35degree using Cryostat Leica CM3050 S (LEICA). For immunofluorescence assay, frozen sections were hydrated with PBS for 10min RT. Antigen was retrieved in citrate buffer (10mM Sodium Citrate, 0.05% Tween 20, pH6.0) for 20min at 100 degree in microwave. Sections were blocked with TBS+2% BSA+5% Donkey serum+0.1%Triton X100 for 1 hr RT, and then stained with primary antibody Rat anti-*Bcl11b* (Abcam), Ki67(Abcam), Krt14 (Covance) overnight, followed by 3X washing by TBST and secondary antibody staining Donkey anti-Rat, rabbit 1:200 (Jackson ImmunoResearch) RT 1hr. After 3X TBST washing and brief DAPI staining (1ug/ml), sections were mounted with Fluoromount® Aqueous Mounting Medium (Sigma). For paraffin section, mammary tissue were fixed by 10% formalin for 2hrs RT and dehydrated by gradient ethanol (70%, 95%,100%) solution. Dehydrated tissue was infiltrated by Xylene solution and embedded with paraffin. Tissue block was sectioned to 10um using Rotary Microtome Leica RM2255 (LEICA). To do the immunofluorescence, paraffin section was de-paraffinized using Xylene and rehydrated with gradient (100%, 95%,70%,0%) ethanol solution and subjected to immunofluorescence staining described above.

Whole Mount—Mammary gland was fixed by Carnoy's fix (60% Ethanol, 30% CHCl3,10% Acetic Acid) for 4hrs. Fixed tissue was washed with a gradient of ethanol (100%, 95%, 70%, 0%), and then stained with carmin-alum staining solution overnight. The next day, tissue was washed with PBS and a gradient of Ethanol (70%, 95%, 100%). Fat tissue was removed by Xylene treatment, and tissue was mounted using Permount® (Fisher Scientific) for long-term preservation.

Transplantation—For Krt14-cre mediated *Bcl11b* knockout transplant assay, isolated mammary cells from 12-week-old *Bcl11b*$^{flox/wt}$ and Krt14-cre *Bcl11b*$^{flox/flox}$ mice were lineage depleted using mammary epithelium enrichment kit (Stem Cells Technologies) according to the manufacturer's instructions. The depletion efficiency and epithelium percentage were determined by flow cytometry. Suspended cells were pelleted and resuspended with injection media (DMEM F12+50% Matrigel+1%PSA) to 50k/5ul, and serially diluted to 25k/5ul, 12.5k/5ul and 2.5k/5ul. Cells were injected as published. 3-week-old NSG recipient mice (Jackson Laboratory) were anesthetized with Ketamine/Xylazine at a dose of 100mg/kg for Ketamine and 10mg/kg for Xylazine. The inguinal rudimentary tree was removed and 5ul of cell suspension was injected onto the residual fat pad using 25ul Hamilton Syringe. Mice were maintained in aseptic sterile condition for 8–12 weeks before whole mount analysis. For secondary transplant, mammary fat pad at 100K dilution, which exclusively gave rise to full tree, were collected and processed to single cell suspension. Mammary epithelia were sorted based on CD24 and CD49f, and 5k epithelia/pad was injected to 3-week-old NSG mice. The MRU frequency and confidence interval were determined by L-Calc (Stem Cell Technologies) or ELDA (http://bioinf.wehi.edu.au/software/elda/).

For Adenovirus-cre mediated *Bcl11b* knockout mammary cells transplant, 8–12 week old *Bcl11b*$^{wt/wt}$ and *Bcl11b*$^{flox/flox}$ mice were lineage depleted using Mammary Epithelium Enrichment Kit (Stem Cell Technologies) and resuspended in culture media (DMEM F12+2%FBS+PSA+10mM HEPES+EGF 10ng/ml+Rspo1 250ng/ml+Noggin 100ng/ml

+Rock inhibitor Y27632 10μM) to 10 million cells/ml/well in 24-well non-adherent culture plate (Corning). Cells were transduced with Adenovirus-cre-GFP (Vector Biolabs) at MOI 10 overnight. The next day, cells were pelleted and treated with 400ul TrypLE^{TM} Select (Gibco)/eppendorf tube at 37 degree for 20mins. Dissociated cells were neutralized with HBSS+2% FBS+PSA and stained with CD45 (Biolegend), CD31 (Biolegend), Ter119 (Biolegend), CD49f (Biolegend), EpCAM (Biolegend). GFP+ epithelia were sorted and then subjected to limiting dilution transplant to NSG recipient mice. Recipient mice were maintained for 10 weeks before analysis. For p53 shRNA and p16 shRNA rescue assay, 50k basal cells/condition from *Bcl11b*$^{flox/flox}$ mouse mammary gland were sorted and transduced with pSIH-GFP control virus, pSIH-GFP-p53shRNA virus and pSIH-GFP-p16shRNA virus respectively at MOI 20, and cultured in 96 well plate at a density 2k/well using the colony formation assay protocol above. Colonies were cultured 7–10 days and dissociated by dispase 1mg/ml (BD Bioscience) for 30min followed by TrypLE^{TM} Select (Gibco) 37degree for 20min to obtain single cells. Single cells were resuspended in 1ml culture media (DMEM F12+2%FBS+PSA+10mM HEPES+EGF 10ng/ml+Rspo1 250ng/ml+Noggin 100ng/ml+Rock inhibitor Y27632 10uM) and transduced by adenovirus-cre-RFP at MOI 10 and cultured in 24-well non-adherent culture plate (Corning) overnight. The next day, cells were pelleted and dissociated with TrypLE^{TM} (Gibson), and GFP and RFP double positive cells were sorted and transplanted to NSG recipient mice with limiting dilution. Mice were maintained for 6–8 weeks before whole mount analysis.

For *Bcl11b*^{high} CD49f^{high}CD24^{med}Lin^{-} single cell transplant assay, mammary gland from 8–12 week old *Bcl11b*$^{td/wt}$ mouse was dissected and processed to single cell suspension, followed by staining and flow cytometry analysis according to the protocol above. *Bcl11b*^{high} CD49f^{high}CD24^{med}Lin^{-} was gated according the tdtomato level of the mature myoepithelial cells. *Bcl11b*^{high} CD49f^{high}CD24^{med}Lin^{-} cells were double sorted to 48-well Terazaki plate (Sigma), containing 5ul culture media/well. Sorted cells were evaluated under the microscope and wells containing single cells were recorded. 5ul matrigel (BD Bioscience) was then added to each well before transplanting to 3-week old C57/BL6 recipient mouse. Recipient mice were maintained for 10 week before whole mount analysis

shRNA knockdown—shRNA against p53 “GTACATGTGTAATAGCTCC” and shRNA against p16 “CATCAAGACATCGTGCGATAT” were cloned into pSIH-GFP Lentiviral vector (Systembio) according to manufacturer’s instructions. Viruses were packaged as described (Adorno et al., 2013). Knockdown efficiency was determined by western blot with Comma D β cell line.

EdU Incorporation Assay—C57/Bl6 mice of 12 week old were injected via IP with 1.25mg/10g EdU. 24hrs after injection, mammary glands were dissected and subjected to EdU label analysis. Click-it reaction and costaining with *Bcl11b* antibody were performed using Click-iT® Assay Kit(Life Technologies) according to manufacturer’s instructions.

PKH26 Long Label Retaining Assay—CD49f^{high}CD24^{med}Lin^{-}was sorted and stained with PKH26 according to manufacturer’s instructions. Specifically, 10k sorted cells were resuspended in 2μM PKH26 and stained for 5mins with periodic mixing before quenching with equal volume of serum. Then stained cells were cultured on growth factor reduced

matrigel with L1 feeder cells for 11days. Colonies were dissociated with dispase (1mg/ml) and trypLE. PKH26 retaining cells and PKH26- cells were sorted by flow cytometer, and then subjected to quantitative real time analysis.

Microarray—pInducer *Bcl11b* Comma D β cell line was treated with 0ng/ml (control) and 100ng/ml Doxycycline overnight. 200k cells from Sca1+ and Sca1- populations of both conditions were sorted. RNA was extracted by RNeasy plus micro kit (Qiagen) according to manufacturer's instructions and quantified by Agilent 2100 Bioanalyzer. Library preparation, hybridization and scanning were all performed by Stanford protein and nucleic acid facility (PAN facility). Affymetrix 3'IVT Express protocol was used to generate biotinylated cRNA from 50–500ngs of total RNA. The fragmented and labeled cRNA was hybridized to mouse genome array MOE430 2.0 with 16hr (overnight) hybridization at 45degC at 60rpm in an Affymetrix GeneChip Hybridization Oven 645. The arrays were then washed and stained in an Affymetrix GeneChip Fluidics Station 450. The arrays were scanned using the Affymetrix GeneChip Scanner 3000 7G. Scanned microarray images were imported into Gene Chip Operating Software (GCOS, Affymetrix) to generate signal values, followed by analysis with BRB-ArrayTools (Biometric Research Branch) using default settings. Heatmap of a collection of genes was generated by Cluster and TreeView (Eisen et al., 1998).

QUANTIFICATION AND STATISTICAL ANALYSIS

The variances between groups were first tested by F-test. Then differences between groups were analyzed using unpaired student's t test with equal variance or unequal variance according to the F-test. Error bars represent standard deviations (± SD) or standard error (±SEM) as indicated in each specific experiment. Each experiment in the paper has been replicated for at least 3 time. In each experiment, N represents the exact times of independent experiments, n represents the sample volume (mouse number, cell number). Statistical parameters and tests are reported in the Figures and corresponding Figure Legends. For limiting dilution analyses, the frequency of mammary repopulating unit was calculated using ELDA software(Hu and Smyth, 2009). Expected frequencies are reported, as well as the 95% confidence intervals (lower and upper values are indicated). No statistical method was used to predetermine sample size, experiments were not randomized and investigators were not blinded to allocation during experiments. Investigators were blinded when assessing outcome of animal experiments (only has ear tag# for identification) during analysis of *Bcl11b* knockout phenotypes. No data or subjects were excluded from the statistical analysis.

DATA AND SOFTWARE AVAILABILITY

Microarray data for induced Bcl11b expression in Comma D beta cells was deposited to GEO with accession code: GSE62059

Supplementary Material

Refer to Web version on PubMed Central for supplementary material.

Acknowledgments

We thank Dr. Mark Leid for providing *Bcl11b*$^{flox/flox}$ mice, Dr. Pentao Liu for providing *Bcl11b*$^{tdtomato/wt}$ reporter mice, Dr. Roel Nusse for providing L1-Wnt3a feeder cells, Dr. Stephen J. Elledge for providing pINDUCER constructs. We also thank Pauline Chu for the help in paraffin section, Patty Lovelace and Jennifer Ho for management of flow cytometry facility, and Andrew Olson for management of NMS Imaging Facility. We thank Stanford PAN facility for microarray analysis. This work was supported by NIH/NCI grant 5P01 CA139490-05, NIH/NCI grant 5U01 CA154209-04, NIH/NCI 5R01 CA100225-09, Department of Defense grant W81XWH-11-1-0287, Department of Defense/Breast Cancer Research Program (BCRP) Innovator Award W81XWH-13-1-0281, The Breast Cancer Research Foundation, the Ludwig Foundation and California Institue of Regenerative Medicine (CIRM) postdoctoral fellowship 1131681-413-UZABP.

References

Adorno M, Sikandar S, Mitra SS, Kuo A, Nicolis Di Robilant B, Haro-Acosta V, Ouadah Y, Quarta M, Rodriguez J, Qian D, et al. Usp16 contributes to somatic stem-cell defects in Down's syndrome. Nature. 2013; 501:380–384. [PubMed: 24025767]

Asselin-Labat ML, Vaillant F, Sheridan JM, Pal B, Wu D, Simpson ER, Yasuda H, Smyth GK, Martin TJ, Lindeman GJ, et al. Control of mammary stem cell function by steroid hormone signalling. Nature. 2010; 465:798–802. [PubMed: 20383121]

Beausejour CM, Krtolica A, Galimi F, Narita M, Lowe SW, Yaswen P, Campisi J. Reversal of human cellular senescence: roles of the p53 and p16 pathways. The EMBO journal. 2003; 22:4212–4222. [PubMed: 12912919]

Behjati S, Huch M, van Boxtel R, Karthaus W, Wedge DC, Tamuri AU, Martincorena I, Petljak M, Alexandrov LB, Gundem G, et al. Genome sequencing of normal cells reveals developmental lineages and mutational processes. Nature. 2014; 513:422–425. [PubMed: 25043003]

Bussard KM, Boulanger CA, Kittrell FS, Behbod F, Medina D, Smith GH. Immortalized, pre-malignant epithelial cell populations contain long-lived, label-retaining cells that asymmetrically divide and retain their template DNA. Breast cancer research : BCR. 2010; 12:R86. [PubMed: 20964820]

Cheng T, Rodrigues N, Shen H, Yang Y, Dombkowski D, Sykes M, Scadden DT. Hematopoietic stem cell quiescence maintained by p21cip1/waf1. Science. 2000; 287:1804–1808. [PubMed: 10710306]

Cismasiu VB, Adamo K, Gecewicz J, Duque J, Lin Q, Avram D. BCL11B functionally associates with the NuRD complex in T lymphocytes to repress targeted promoter. Oncogene. 2005; 24:6753–6764. [PubMed: 16091750]

Codega P, Silva-Vargas V, Paul A, Maldonado-Soto AR, Deleo AM, Pastrana E, Doetsch F. Prospective identification and purification of quiescent adult neural stem cells from their in vivo niche. Neuron. 2014; 82:545–559. [PubMed: 24811379]

Dalerba P, Kalisky T, Sahoo D, Rajendran PS, Rothenberg ME, Leyrat AA, Sim S, Okamoto J, Johnston DM, Qian D, et al. Single-cell dissection of transcriptional heterogeneity in human colon tumors. Nature biotechnology. 2011; 29:1120–1127.

Deugnier MA, Faraldo MM, Teuliere J, Thiery JP, Medina D, Glukhova MA. Isolation of mouse mammary epithelial progenitor cells with basal characteristics from the Comma-Dbeta cell line. Developmental biology. 2006; 293:414–425. [PubMed: 16545360]

dos Santos CO, Rebbeck C, Rozhkova E, Valentine A, Samuels A, Kadiri LR, Osten P, Harris EY, Uren PJ, Smith AD, et al. Molecular hierarchy of mammary differentiation yields refined markers of mammary stem cells. Proceedings of the National Academy of Sciences of the United States of America. 2013; 110:7123–7130. [PubMed: 23580620]

Eisen MB, Spellman PT, Brown PO, Botstein D. Cluster analysis and display of genome-wide expression patterns. Proceedings of the National Academy of Sciences of the United States of America. 1998; 95:14863–14868. [PubMed: 9843981]

Essers MA, Offner S, Blanco-Bose WE, Waibler Z, Kalinke U, Duchosal MA, Trumpp A. IFNalpha activates dormant haematopoietic stem cells in vivo. Nature. 2009; 458:904–908. [PubMed: 19212321]

Foudi A, Hochedlinger K, Van Buren D, Schindler JW, Jaenisch R, Carey V, Hock H. Analysis of histone 2B-GFP retention reveals slowly cycling hematopoietic stem cells. Nature biotechnology. 2009; 27:84–90.

Fuchs E. The tortoise and the hair: slow-cycling cells in the stem cell race. Cell. 2009; 137:811–819. [PubMed: 19490891]

Golonzhka O, Liang X, Messaddeq N, Bornert JM, Campbell AL, Metzger D, Chambon P, Ganguli-Indra G, Leid M, Indra AK. Dual role of COUP-TF-interacting protein 2 in epidermal homeostasis and permeability barrier formation. The Journal of investigative dermatology. 2009; 129:1459–1470. [PubMed: 19092943]

Gothot A, Pyatt R, McMahel J, Rice S, Srour EF. Functional heterogeneity of human CD34(+) cells isolated in subcompartments of the G0 /G1 phase of the cell cycle. Blood. 1997; 90:4384–4393. [PubMed: 9373249]

Harmes DC, DiRenzo J. Cellular quiescence in mammary stem cells and breast tumor stem cells: got testable hypotheses? Journal of mammary gland biology and neoplasia. 2009; 14:19–27. [PubMed: 19240987]

Hu Y, Smyth GK. ELDA: extreme limiting dilution analysis for comparing depleted and enriched populations in stem cell and other assays. Journal of immunological methods. 2009; 347:70–78. [PubMed: 19567251]

Jamieson CH, Ailles LE, Dylla SJ, Muijtjens M, Jones C, Zehnder JL, Gotlib J, Li K, Manz MG, Keating A, et al. Granulocyte-macrophage progenitors as candidate leukemic stem cells in blast-crisis CML. The New England journal of medicine. 2004; 351:657–667. [PubMed: 15306667]

Jan M, Snyder TM, Corces-Zimmerman MR, Vyas P, Weissman IL, Quake SR, Majeti R. Clonal evolution of preleukemic hematopoietic stem cells precedes human acute myeloid leukemia. Science translational medicine. 2012; 4:149ra118.

Joshi PA, Jackson HW, Beristain AG, Di Grappa MA, Mote PA, Clarke CL, Stingl J, Waterhouse PD, Khokha R. Progesterone induces adult mammary stem cell expansion. Nature. 2010; 465:803–807. [PubMed: 20445538]

Khaled WT, Choon Lee S, Stingl J, Chen X, Raza Ali H, Rueda OM, Hadi F, Wang J, Yu Y, Chin SF, et al. BCL11A is a triple-negative breast cancer gene with critical functions in stem and progenitor cells. Nature communications. 2015; 6:5987.

Kippin TE, Martens DJ, van der Kooy D. p21 loss compromises the relative quiescence of forebrain stem cell proliferation leading to exhaustion of their proliferation capacity. Genes & development. 2005; 19:756–767. [PubMed: 15769947]

Krasteva V, Buscarlet M, Diaz-Tellez A, Bernard MA, Crabtree GR, Lessard JA. The BAF53a subunit of SWI/SNF-like BAF complexes is essential for hemopoietic stem cell function. Blood. 2012; 120:4720–4732. [PubMed: 23018638]

Krishnamurthy J, Ramsey MR, Ligon KL, Torrice C, Koh A, Bonner-Weir S, Sharpless NE. p16INK4a induces an age-dependent decline in islet regenerative potential. Nature. 2006; 443:453–457. [PubMed: 16957737]

Li P, Burke S, Wang J, Chen X, Ortiz M, Lee SC, Lu D, Campos L, Goulding D, Ng BL, et al. Reprogramming of T cells to natural killer-like cells upon Bcl11b deletion. Science. 2010; 329:85–89. [PubMed: 20538915]

Lin AW, Barradas M, Stone JC, van Aelst L, Serrano M, Lowe SW. Premature senescence involving p53 and p16 is activated in response to constitutive MEK/MAPK mitogenic signaling. Genes & development. 1998; 12:3008–3019. [PubMed: 9765203]

Liu H, Adler AS, Segal E, Chang HY. A transcriptional program mediating entry into cellular quiescence. PLoS genetics. 2007; 3:e91. [PubMed: 17559306]

Marques-Torrejon MA, Porlan E, Banito A, Gomez-Ibarlucea E, Lopez-Contreras AJ, Fernandez-Capetillo O, Vidal A, Gil J, Torres J, Farinas I. Cyclin-dependent kinase inhibitor p21 controls adult neural stem cell expansion by regulating Sox2 gene expression. Cell stem cell. 2013; 12:88–100. [PubMed: 23260487]

Matsumoto A, Takeishi S, Kanie T, Susaki E, Onoyama I, Tateishi Y, Nakayama K, Nakayama KI. p57 is required for quiescence and maintenance of adult hematopoietic stem cells. Cell stem cell. 2011; 9:262–271. [PubMed: 21885021]

Park IK, Qian D, Kiel M, Becker MW, Pihalja M, Weissman IL, Morrison SJ, Clarke MF. Bmi-1 is required for maintenance of adult self-renewing haematopoietic stem cells. Nature. 2003; 423:302–305. [PubMed: 12714971]

Pece S, Tosoni D, Confalonieri S, Mazzarol G, Vecchi M, Ronzoni S, Bernard L, Viale G, Pelicci PG, Di Fiore PP. Biological and molecular heterogeneity of breast cancers correlates with their cancer stem cell content. Cell. 2010; 140:62–73. [PubMed: 20074520]

Pietersen AM, Evers B, Prasad AA, Tanger E, Cornelissen-Steijger P, Jonkers J, van Lohuizen M. Bmi1 regulates stem cells and proliferation and differentiation of committed cells in mammary epithelium. Current biology : CB. 2008; 18:1094–1099. [PubMed: 18635350]

Plaks V, Brenot A, Lawson DA, Linnemann JR, Van Kappel EC, Wong KC, de Sauvage F, Klein OD, Werb Z. Lgr5-expressing cells are sufficient and necessary for postnatal mammary gland organogenesis. Cell reports. 2013; 3:70–78. [PubMed: 23352663]

Prater M, Shehata M, Watson CJ, Stingl J. Enzymatic dissociation, flow cytometric analysis, and culture of normal mouse mammary tissue. Methods in molecular biology. 2013; 946:395–409. [PubMed: 23179846]

Prater MD, Petit V, Alasdair Russell I, Giraddi RR, Shehata M, Menon S, Schulte R, Kalajzic I, Rath N, Olson MF, et al. Mammary stem cells have myoepithelial cell properties. Nature cell biology. 2014; 16:942–950. 941–947. [PubMed: 25173976]

Pustavoitau A, Barodka V, Sharpless NE, Torrice C, Nyhan D, Berkowitz DE, Shah AS, Bandeen Roche KJ, Walston JD. Role of senescence marker p16(INK4a) measured in peripheral blood T-lymphocytes in predicting length of hospital stay after coronary artery bypass surgery in older adults. Experimental gerontology. 2016; 74:29–36. [PubMed: 26692418]

Rios AC, Fu NY, Lindeman GJ, Visvader JE. In situ identification of bipotent stem cells in the mammary gland. Nature. 2014; 506:322–327. [PubMed: 24463516]

Russell TD, Fischer A, Beeman NE, Freed EF, Neville MC, Schaack J. Transduction of the mammary epithelium with adenovirus vectors in vivo. Journal of virology. 2003; 77:5801–5809. [PubMed: 12719573]

Sahoo D, Dill DL, Gentles AJ, Tibshirani R, Plevritis SK. Boolean implication networks derived from large scale, whole genome microarray datasets. Genome biology. 2008; 9:R157. [PubMed: 18973690]

Sato S, Kawamata Y, Takahashi A, Imai Y, Hanyu A, Okuma A, Takasugi M, Yamakoshi K, Sorimachi H, Kanda H, et al. Ablation of the p16(INK4a) tumour suppressor reverses ageing phenotypes of klotho mice. Nature communications. 2015; 6:7035.

Schmidt M, Fernandez de Mattos S, van der Horst A, Klompmaker R, Kops GJ, Lam EW, Burgering BM, Medema RH. Cell cycle inhibition by FoxO forkhead transcription factors involves downregulation of cyclin D. Molecular and cellular biology. 2002; 22:7842–7852. [PubMed: 12391153]

Schmitt CA, Fridman JS, Yang M, Lee S, Baranov E, Hoffman RM, Lowe SW. A senescence program controlled by p53 and p16INK4a contributes to the outcome of cancer therapy. Cell. 2002; 109:335–346. [PubMed: 12015983]

Shackleton M, Vaillant F, Simpson KJ, Stingl J, Smyth GK, Asselin-Labat ML, Wu L, Lindeman GJ, Visvader JE. Generation of a functional mammary gland from a single stem cell. Nature. 2006; 439:84–88. [PubMed: 16397499]

Sharpless NE. Ink4a/Arf links senescence and aging. Experimental gerontology. 2004; 39:1751–1759. [PubMed: 15582292]

Shimono Y, Zabala M, Cho RW, Lobo N, Dalerba P, Qian D, Diehn M, Liu H, Panula SP, Chiao E, et al. Downregulation of miRNA-200c links breast cancer stem cells with normal stem cells. Cell. 2009; 138:592–603. [PubMed: 19665978]

Smith GH. Label-retaining epithelial cells in mouse mammary gland divide asymmetrically and retain their template DNA strands. Development. 2005; 132:681–687. [PubMed: 15647322]

Spencer SL, Cappell SD, Tsai FC, Overton KW, Wang CL, Meyer T. The proliferation-quiescence decision is controlled by a bifurcation in CDK2 activity at mitotic exit. Cell. 2013; 155:369–383. [PubMed: 24075009]

Stingl J, Eirew P, Ricketson I, Shackleton M, Vaillant F, Choi D, Li HI, Eaves CJ. Purification and unique properties of mammary epithelial stem cells. Nature. 2006; 439:993–997. [PubMed: 16395311]

van Amerongen R, Bowman AN, Nusse R. Developmental stage and time dictate the fate of Wnt/beta-catenin-responsive stem cells in the mammary gland. Cell stem cell. 2012; 11:387–400. [PubMed: 22863533]

Van Keymeulen A, Rocha AS, Ousset M, Beck B, Bouvencourt G, Rock J, Sharma N, Dekoninck S, Blanpain C. Distinct stem cells contribute to mammary gland development and maintenance. Nature. 2011; 479:189–193. [PubMed: 21983963]

Wang D, Cai C, Dong X, Yu QC, Zhang XO, Yang L, Zeng YA. Identification of multipotent mammary stem cells by protein C receptor expression. Nature. 2015; 517:81–84. [PubMed: 25327250]

Wilson A, Laurenti E, Oser G, van der Wath RC, Blanco-Bose W, Jaworski M, Offner S, Dunant CF, Eshkind L, Bockamp E, et al. Hematopoietic stem cells reversibly switch from dormancy to self-renewal during homeostasis and repair. Cell. 2008; 135:1118–1129. [PubMed: 19062086]

Zeng YA, Nusse R. Wnt proteins are self-renewal factors for mammary stem cells and promote their long-term expansion in culture. Cell stem cell. 2010; 6:568–577. [PubMed: 20569694]

Zou P, Yoshihara H, Hosokawa K, Tai I, Shinmyozu K, Tsukahara F, Maru Y, Nakayama K, Nakayama KI, Suda T. p57(Kip2) and p27(Kip1) cooperate to maintain hematopoietic stem cell quiescence through interactions with Hsc70. Cell stem cell. 2011; 9:247–261. [PubMed: 21885020]

Reference

Adorno M, Sikandar S, Mitra SS, Kuo A, Nicolis Di Robilant B, Haro-Acosta V, Ouadah Y, Quarta M, Rodriguez J, Qian D, et al. Usp16 contributes to somatic stem-cell defects in Down's syndrome. Nature. 2013; 501:380–384. [PubMed: 24025767]

Campbell SM, Taha MM, Medina D, Rosen JM. A clonal derivative of mammary epithelial cell line COMMA-D retains stem cell characteristics of unique morphological and functional heterogeneity. Experimental cell research. 1988; 177:109–121. [PubMed: 2455648]

Dalerba P, Kalisky T, Sahoo D, Rajendran PS, Rothenberg ME, Leyrat AA, Sim S, Okamoto J, Johnston DM, Qian D, et al. Single-cell dissection of transcriptional heterogeneity in human colon tumors. Nature biotechnology. 2011; 29:1120–1127.

Eisen MB, Spellman PT, Brown PO, Botstein D. Cluster analysis and display of genome-wide expression patterns. Proceedings of the National Academy of Sciences of the United States of America. 1998; 95:14863–14868. [PubMed: 9843981]

Golonzhka O, Liang X, Messaddeq N, Bornert JM, Campbell AL, Metzger D, Chambon P, Ganguli-Indra G, Leid M, Indra AK. Dual role of COUP-TF-interacting protein 2 in epidermal homeostasis and permeability barrier formation. The Journal of investigative dermatology. 2009; 129:1459–1470. [PubMed: 19092943]

Hu Y, Smyth GK. ELDA: extreme limiting dilution analysis for comparing depleted and enriched populations in stem cell and other assays. Journal of immunological methods. 2009; 347:70–78. [PubMed: 19567251]

Li P, Burke S, Wang J, Chen X, Ortiz M, Lee SC, Lu D, Campos L, Goulding D, Ng BL, et al. Reprogramming of T cells to natural killer-like cells upon Bcl11b deletion. Science. 2010; 329:85–89. [PubMed: 20538915]

Prater M, Shehata M, Watson CJ, Stingl J. Enzymatic dissociation, flow cytometric analysis, and culture of normal mouse mammary tissue. Methods in molecular biology. 2013; 946:395–409. [PubMed: 23179846]

Highlights

- A subset of mammary basal epithelial cells express high levels of *Bcl11b*
- Loss of *Bcl11b* impairs mammary gland development and regenerative capacity
- *Bcl11b*^{high} cells are quiescent but have potent regenerative activity in transplants
- *Bcl11b* interacts with cell cycle regulators to induce a quiescent state

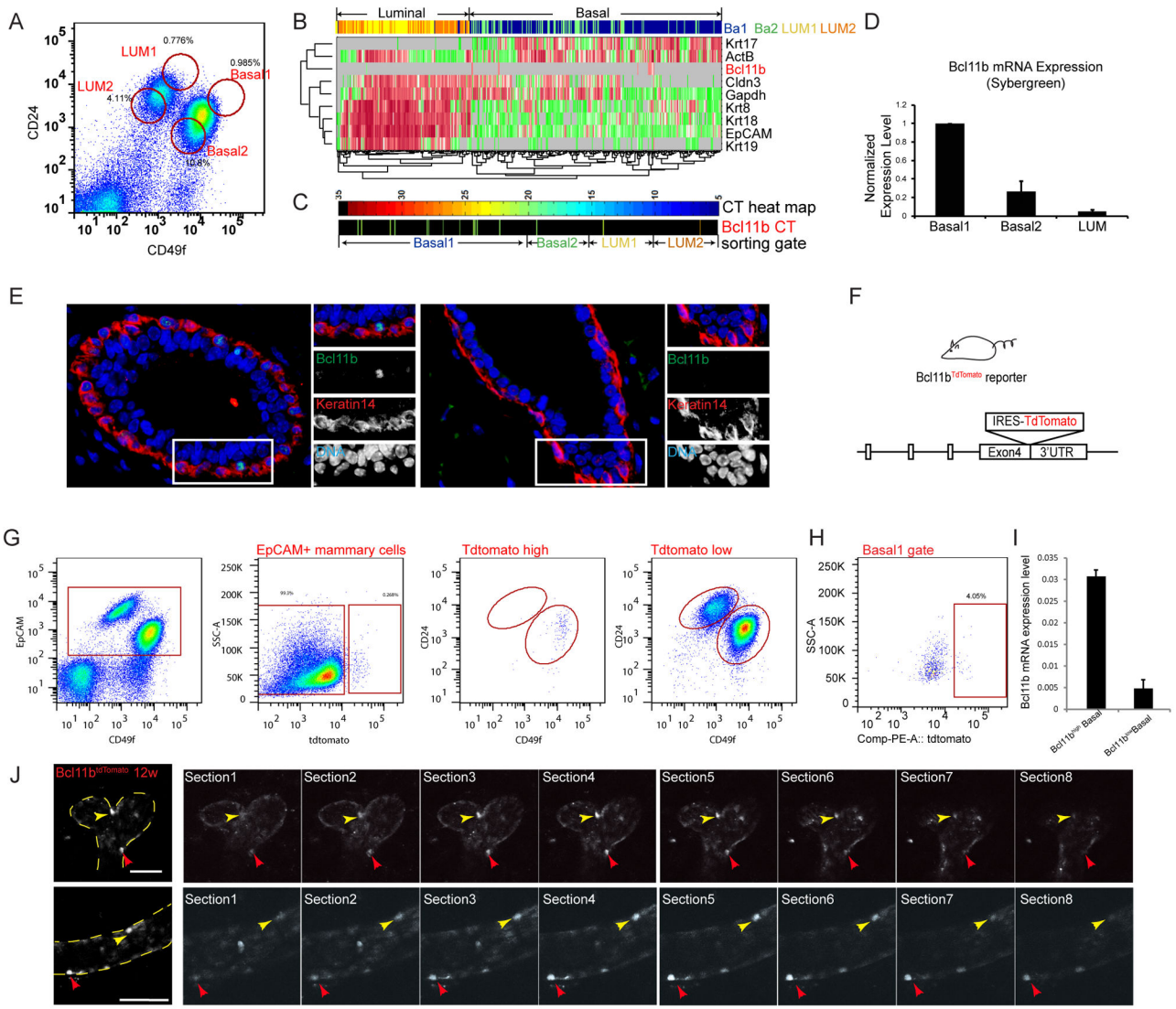

Fig 1. *Bcl11b* expression is restricted to CD49f^{high}CD24^{med}Lineage^{-} cells and shows sporadic localization in the basal layer

(**A**) FACS plot of a mammary gland from an 8–12 week old adult mouse with surface markers CD24 and CD49f. Red circles show gates for Basal1(CD49f^{high}CD24^{med}Lineage^{-}), Basal2(CD49f^{high}CD24^{low}Lineage^{-}), LUM1(CD49f^{low}CD24^{high}Lineage^{-}) and LUM2(CD49f^{low}CD24^{low}Lineage^{-}) populations. (**B,C**) Single cell gene expression analysis of *Bcl11b* in Basal1, Basal2 and Luminal cells. Cell and gene clustering are superimposed with the expression panel in (**B**). Red color indicates high expression, green indicates low expression and gray indicates no expression. The Ct value of *Bcl11b* in the original gates is shown in (**C**). In this scale bar, blue color indicates low Ct value (high expression), while red color indicates high Ct value (low expression). (**D**) Real time PCR quantification of *Bcl11b* mRNA levels in Basal1, Basal2 and Luminal cells with ActB as an internal control. Data were presented as Mean±SEM. N=3 (**E**) Immunofluorescence of the mammary gland from an 8 week old mouse. Red: Krt14; Green: *Bcl11b*; Blue: DAPI. Scale bar, 20μm (**F**) Schematic diagram of *Bcl11b* tdTomato reporter mouse. (**G**) A representative FACS plot of

a mammary gland from a *Bcl11b*$^{tdtomato/wt}$ reporter mouse. The TdTomato expression level is shown for EpCAM+ mammary cells. (**H**) Tdtomato expression level is shown for CD49f^{high}CD24^{med}Lineage^{-} population. (**I**) Real time PCR confirming *Bcl11b*^{high} population isolated from *Bcl11b* tdtomato reporter mice enriched for *Bcl11b* mRNA expression. N=3, $p<0.01$. (**J**) Mammary bifurcating mammary duct of a 12-week-old *Bcl11b*$^{tdtomato/wt}$ mouse. Stacked images were shown on the left panel. Optical sections were shown on the right panel. Yellow arrowheads point to individual tdTomato positive cells. Scale bar, 100μm. See also Figure S1

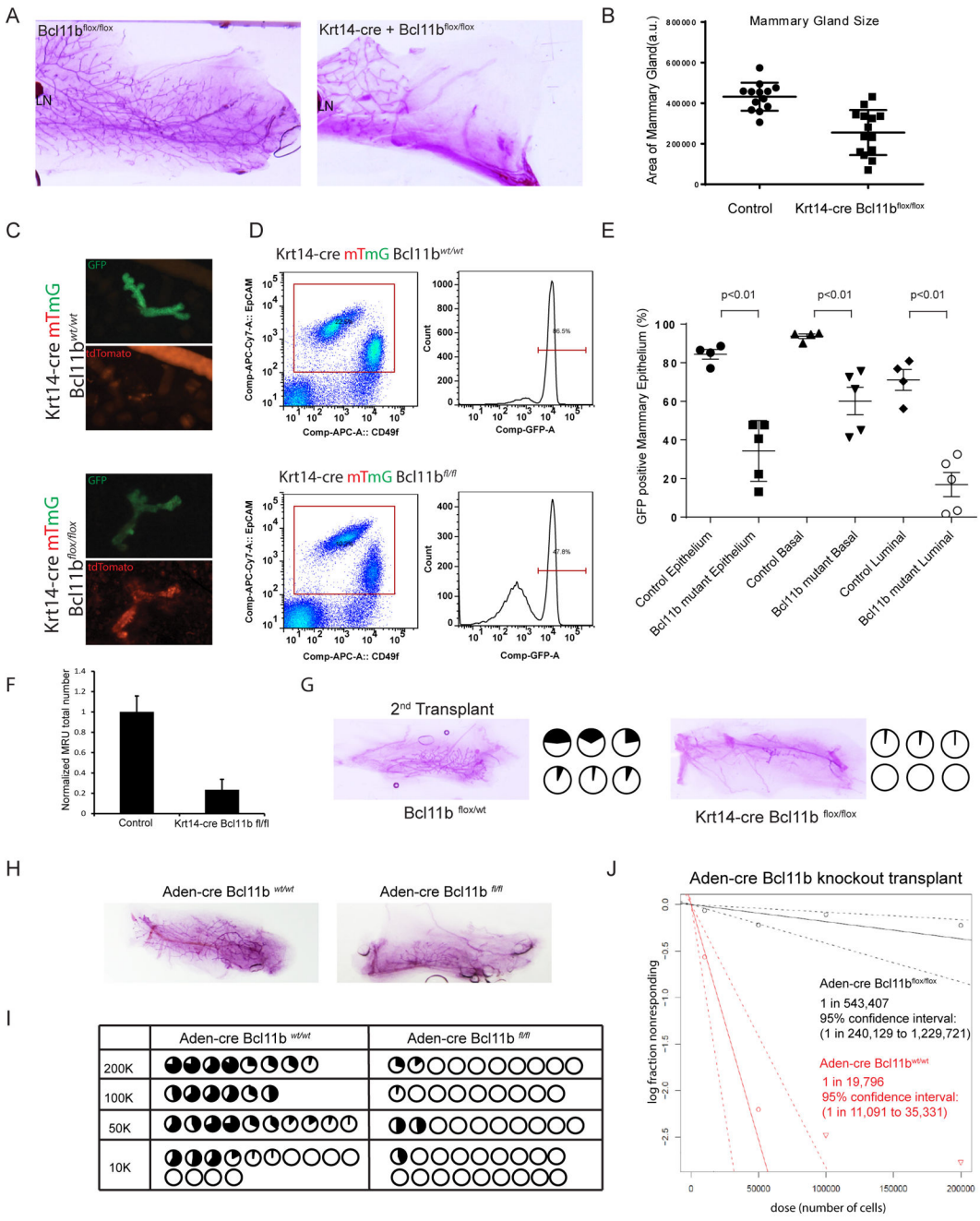

Fig. 2. Deletion of *Bcl11b* causes mammary gland hypoplasia

(**A**) Whole mount image of *Bcl11b*$^{flox/flox}$ and Krt14-cre *Bcl11b*$^{flox/flox}$ inguinal mammary gland at week 9. (**B**) Quantification of mammary gland size from littermates (control and *Bcl11b* mutant) at adulthood (10–14 weeks). Data are plotted as Mean±S.D. ($p<0.0001$, n=16). (**C**) Image of collagenase digested mammary gland fragments from Krt14-cre mTmG *Bcl11b*$^{wt/wt}$ and Krt14-cre mTmG *Bcl11b*$^{flox/flox}$ mice showing GFP and tdTomato. (**D**) FACS analysis of Krt14-cre mTmG *Bcl11b*$^{wt/wt}$ and Krt14-cre mTmG *Bcl11b*$^{flox/flox}$ mice with CD49f and EpCAM. EpCAM positive mammary epithelia were gated and plotted using GFP. (**E**) Quantification of GFP positive cells of whole mammary epithelia, basal cells and

luminal cells. Data were presented as mean±SD. (n=5) **(F)** Total MRU number quantified by limiting dilution transplantation of lineage negative mammary cells from control and Krt14-cre *Bcl11b*$^{flox/flox}$ mice. Data were normalized to the control MRU number. n=3, $p<0.01$ (**G**) Images and pie chart of the secondary transplant of the mammary outgrowths from control and Krt14-cre *Bcl11b*$^{flox/flox}$ mice. (**H**) Whole mount images of control (adeno-cre *Bcl11b*$^{wt/wt}$) and mutant (adeno-cre *Bcl11b*$^{flox/flox}$) transplants. (**I**) Pie chart of limiting dilution transplant of adenovirus-cre mediated *Bcl11b* knockout mammary epithelia. (**J**) ELDA plot of limiting dilution transplant of adenovirus-cre mediated *Bcl11b* knockout mammary epithelia. N=3, $p<0.01$. See also figure S2.

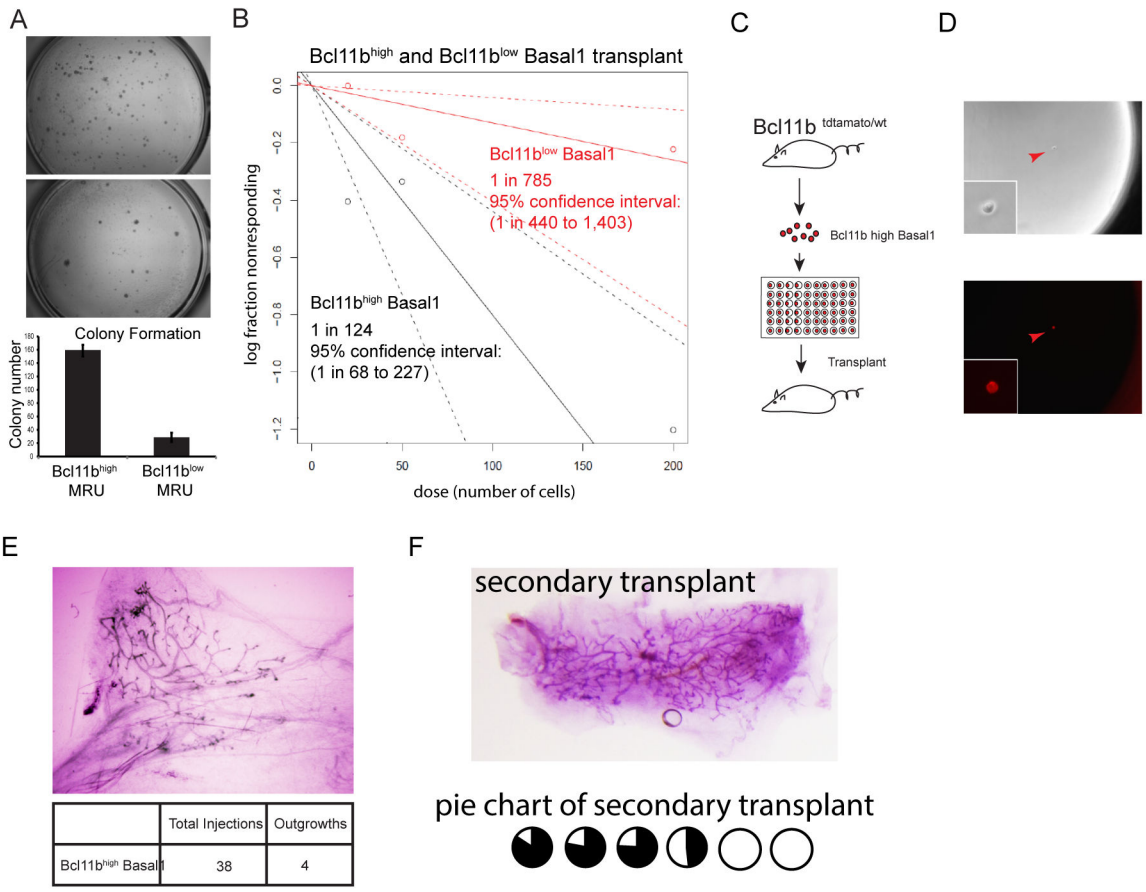

Fig. 3. Cells expressing high levels of *Bcl11b* are enriched for CD49f^{high}CD24^{med}Lineage^{-} cells

(**A**) Colony formation assay for CD49f^{high}CD24^{med}Lin^{-} expressing high versus low levels of *Bcl11b*. 1K cells/well were seeded for each condition and cultured for a week. Number of colonies were counted and plotted in the bar graph. The data are presented as mean ±S.E.M (N=3, p<0.01) (**B**) ELDA plot of Limiting dilution transplant of the *Bcl11b*^{high} and *Bcl11b*^{low} CD49f^{high}CD24^{med}Lineage^{-} populations (**C,D,E**) Single cell transplants of *Bcl11b*^{high} CD49f^{high}CD24^{med}Lineage^{-} cells. A schematic diagram of single cell sorting and a representative *Bcl11b*^{high} single cell image in a Terasaki plate is shown in (**C,D**). A whole mount image of a representative singe cell transplant outgrowth is shown in (**E**) with the table showing the numbers of total injections and outgrowths (**E**). (**F**) The mammary outgrowths from *Bcl11b*^{high}CD49f ^{high}CD24^{med}lin^{-} cells were dissected and dissociated to single cells. Single cell suspensions from two distinct mammary outgrowths were passaged to 6 recipient mice for secondary transplant. Pie chart shows the tree coverage of the mammary fat pad. See also Figure S3.

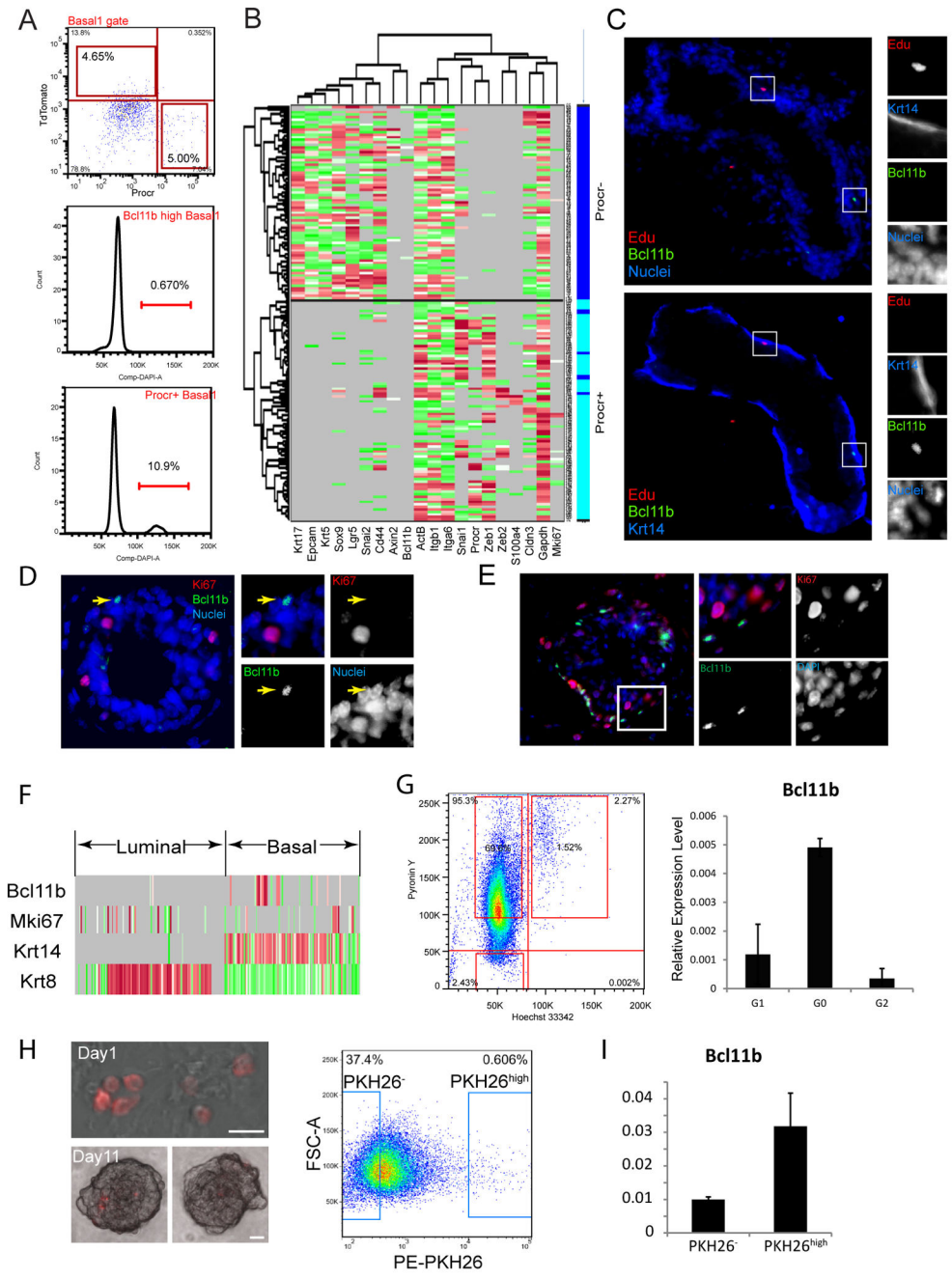

Fig. 4. *Bcl11b*^{high} cells in mammary gland are quiescent

(A) Flow plot showing *Bcl11b*^{high} cells are distinct from Procr+ cells within CD49f^{high}CD24^{med}Lin^{-}gate. DNA content analysis of *Bcl11b*^{high} and procr+ CD49f^{high}CD24^{med}Lin^{-}. Procr+ CD49f^{high}CD24^{med}Lin^{-}contained more proliferating cells (11%) than *Bcl11b*^{high} CD49f^{high}CD24^{med}Lin^{-} (0.67%). (**B**) Single cell gene expression analysis of Procr+ and Procr- basal cells. (**C**) EdU incorporation assay for *Bcl11b*^{high} cells. Adult mice (8–12weeks) were injected via IP with 1.25mg/20g EdU for one day and analyzed for Edu incorporation (red), *Bcl11b* (green), Krt14 (blue) 24 hrs later. (**D,E**) Immunofluorescence co-staining of *Bcl11b* and Ki67 in mammary gland frozen sections

from a pubescent mouse showing mammary ducts and terminal end bud. Green: *Bcl11b*. Red: Ki67. Blue: DAPI (**F**) Single cell gene expression analysis showing that the mRNA expressions of *Bcl11b* and Ki67 are mutually exclusive. (**G**) Left panel: $CD49f^{high}CD24^{med}Lineage^{-}$ cells were sorted and stained with Pyronin Y and Hoechst 33342. The G_0, G1 and SG_2M cells were sorted and subjected to real time PCR. Right panel: real time PCR analysis of *Bcl11b* expression level in various cell populations. N=3 (**H**) Images showing day1 and day11 culture of PKH26 stained $CD49f^{high}CD24^{med}Lineage^{-}$ cells, and sorting gates of PKH26 retaining and non-retaining cells. (**I**) Real time quantification of *Bcl11b* expression in the PKH26 retaining ($PKH26^{high}$) and PKH26 low ($PKH26^{-}$) populations. Data are presented as mean ±S.E.M (N=4, $p<0.05$). See also Figure S4

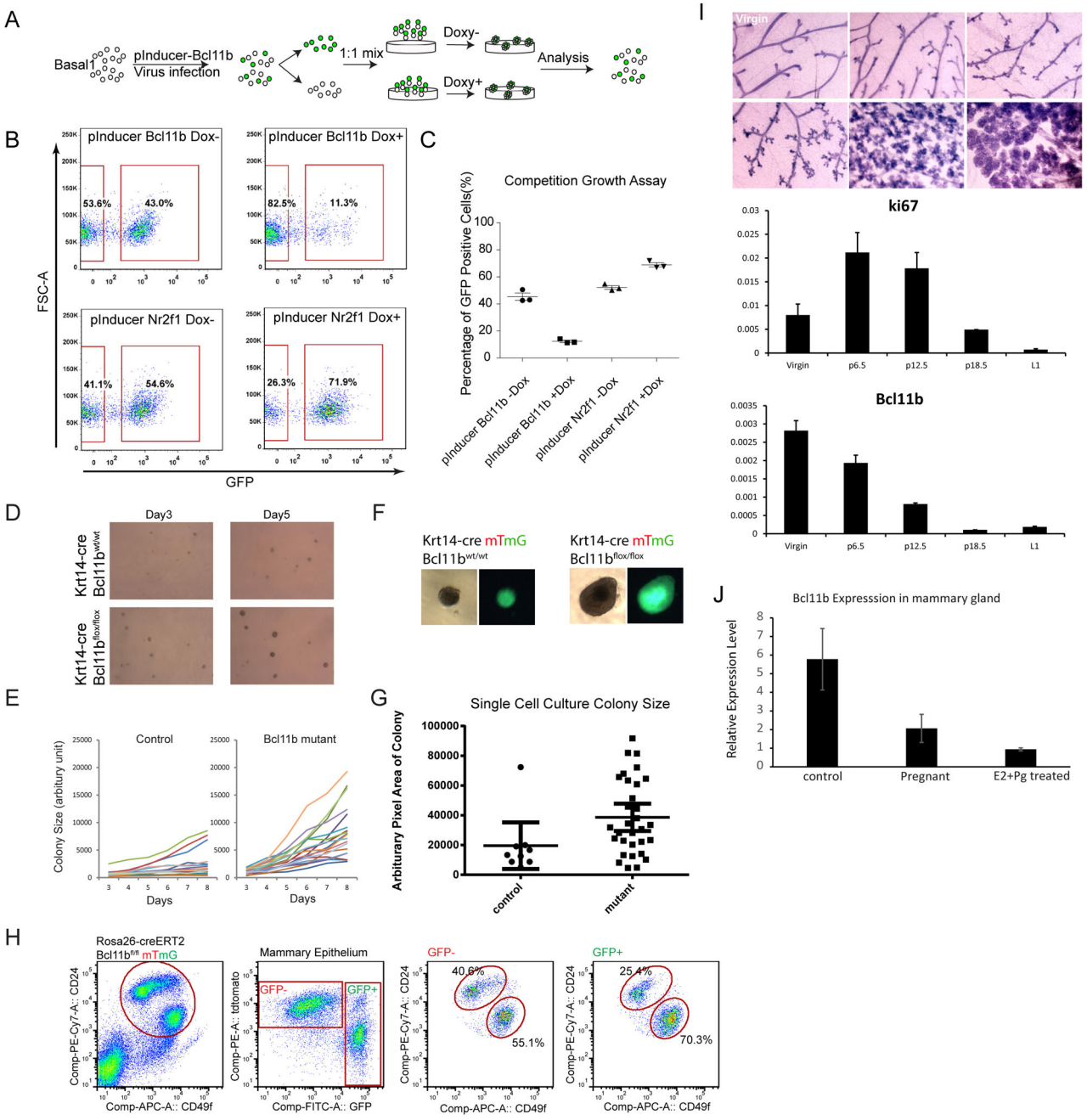

Fig. 5. *Bcl11b* functionally regulates mammary epithelial cells

(**A**) Schematic diagram showing the strategy of the competition growth assay. Sorted CD49f^{high}CD24^{med}Lineage^{-} cells were infected with a *Bcl11b* inducible construct. Infected cells (GFP+) and uninfected cells (GFP−) were mixed in a 1:1 ratio and cultured in the absence (Dox−) or presence (Dox+) of Doxycycline. Colonies were digested to single cells and analyzed by flow cytometry. (**B**) Competition growth assay with induced *Bcl11b* or Nr2f1 in the presence or absence of 100ng/ml Doxycycline for 3 days (**C**) Quantification of GFP percentage in *Bcl11b* or Nr2f1 competition growth assay. Data are presented as mean ±S.D. (N=3). (**D**) Images of the colonies arising from CD49f^{high}CD24^{med}Lineage^{-} cells in a

3D culture from Krt14-cre *Bcl11b*$^{wt/wt}$ and Krt14-cre *Bcl11b*$^{flox/flox}$ mice. Images on day3 and day5 are shown. (**E**) The colony size of each individual colony was quantified and plotted over time. (**F,G**) Quantification of the sizes of colonies in a single cell culture assay from Krt14-cre *Bcl11b*$^{wt/wt}$ and Krt14-cre *Bcl11b*$^{flox/flox}$ mice. Single CD49f^{high}CD24^{med}Lineage^{-} cells were sorted to 96-well plates (1cell/well) and cultured for colony formation. Data are presented as mean ±S.D. ($p<0.05$) (**H**) Induced deletion of *Bcl11b* with a Rosa26-creERT2 *Bcl11b*$^{flox/flox}$ mTmG mouse. 8 week-old Rosa26-creERT2 *Bcl11b*$^{flox/flox}$ mTmG mouse was administered with one dose 1mg/10g tamoxifen and left in husbandry for 3 weeks. Mammary glands were dissected and analyzed by flow cytometry. (**I**) Gene expression analysis of mouse basal cells at different stages of mouse pregnancy. Mammary glands from mice at different pregnancy stages p0, p6.5, p12.5, p18.5, lactation L1, were harvested and dissociated into single cells. Sorted basal cells were subjected to real time PCR analysis. (**J**) Hormone regulation of Bcl11b expression in mammary gland. Adult mice were ovariectomized and treated with vehicle (corn oil) or Estrogen (10ug) +Progesterone (1mg). Bcl11b expression was quantified by real time PCR, compared with pregnant mammary gland at stage p12.5. N=3 See also Figure S5,6.

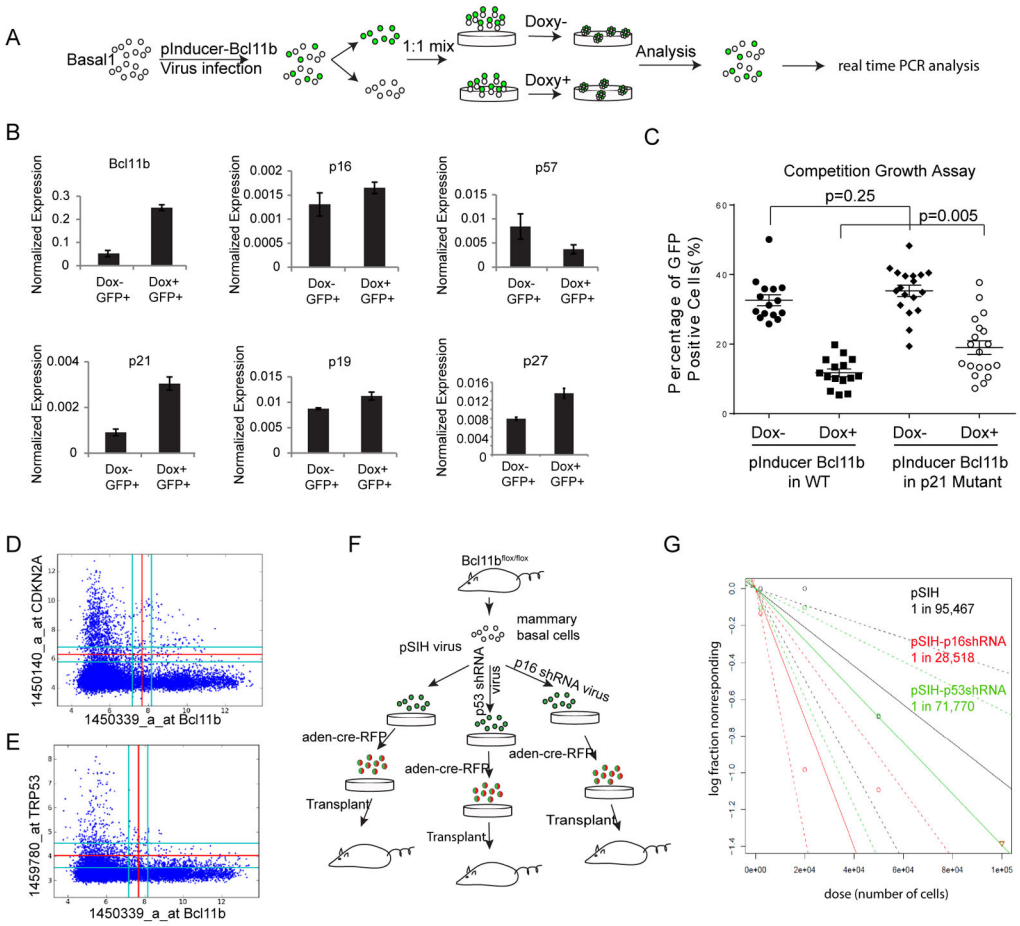

Fig. 6. *Bcl11b* regulation of CD49f^{high}CD24^{med}Lineage^{-} proliferation and engraftment via Cdkn1a(p21) and Cdkn2a(p16)

(A) Schematic Diagram showing the process of real time PCR analysis of *Bcl11b* induced and uninduced populations in colonies formed by CD49f^{high}CD24^{med}Lin^{-}. **(B)** mRNA expression levels of selected CDKIs (p21, p16, p19, p27, p57) after induced *Bcl11b* expression in CD49f^{high}CD24^{med}Lineage^{-} cells in 3D culture. GFP+ cells from Dox- (0ng/ml) and Dox+(50ng/ml) samples were sorted for real time gene expression analysis. (**C**) Competition growth assay with *Bcl11b* induction in p21 knockout mice. Note: p21 knockout partially rescues *Bcl11b*-mediated repression of proliferation. N=3 (**D**) Gene expression plot of Cdkn2a(p16) versus *Bcl11b* from the currently available 10,000 mouse microarrays. Each dot represents one microarray dataset. (**E**) Gene expression plot of p53 versus *Bcl11b* from the currently available 10,000 mouse microarrays. Each dot represents one microarray dataset. (**F**) Schematic diagram showing the design of the p16 shRNA and p53 shRNA rescue assays. Basal1 cells from *Bcl11b$^{flox/flox}$* mice were sorted and transduced with p16 or p53 shRNA lentivirus and cultured for a week on 3D matrigel. Mammary colonies were then dissociated and transduced with adeno-cre-RFP and cultured overnight. The GFP and RFP double positive cells were then sorted and transplanted into NSG recipient mice. (**G**) Limiting dilution transplants of adeno-cre mediated *Bcl11b* knockout basal cells infected with p16 shRNA or p53 shRNA vectors. In contrast to p53 shRNA,

which did not show significant difference in repopulation frequency, p16 shRNA did rescue the engraftment by ~3 fold. (N=3, P_{pSIH} vs p16 shRNA<0.05, $P_{pSIH\ vs\ p53shRNA}$=0.63).